THE DEVELOPMENT OF CORRELATIONS BETWEEN HMA PAVEMENT PERFORMANCE AND AGGREGATE SHAPE PROPERTIES

A Thesis

by

JEREMY MCGAHAN

Submitted to the Office of Graduate Studies of
Texas A&M University
in partial fulfillment of the requirements for the degree of

MASTER OF SCIENCE

December 2005

Major Subject: Civil Engineering

THE DEVELOPMENT OF CORRELATIONS BETWEEN HMA PAVEMENT PERFORMANCE AND AGGREGATE SHAPE PROPERTIES

A Thesis

by

JEREMY MCGAHAN

Submitted to the Office of Graduate Studies of
Texas A&M University
in partial fulfillment of the requirements for the degree of

MASTER OF SCIENCE

Approved by:

Chair of Committee,	Eyad Masad
Committee Members,	Amy Epps-Martin
	Cliff Spiegelman
Head of Department,	David Rosowsky

December 2005

Major Subject: Civil Engineering

ABSTRACT

The Development of Correlations Between HMA Pavement Performance and Aggregate Shape Properties. (December 2005)

Jeremy McGahan, B.S., Texas A&M University

Chair of Advisory Committee: Dr. Eyad Masad

The physical characteristics of aggregates (form, angularity, and texture) are known to affect the performance of hot mix asphalt (HMA) pavements. Efforts to develop relationships between these aggregate characteristics and aggregate performance in HMA pavements have been limited in the past due to inherent inaccuracies in the methods used to measure these characteristics. The recently developed Aggregate Imaging System (AIMS) offers an opportunity to accurately measure aggregate shape characteristics allowing them to be properly related to asphalt performance.

This research focused on relating the aggregate characteristics of form, angularity, and texture measured using AIMS to laboratory performance measurements on a wide variety of HMA mixes. The performance of these mixes was evaluated in three projects carried out by the Federal Highway Administration (FHWA) and the Texas Transportation Institute (TTI). During this research, a database of the volumetric, performance, and aggregate shape measurements for mixes used in these projects was created. Statistical analysis was conducted to correlate HMA performance parameters to volumetric and aggregate shape characteristics. The results show the dominant effect that aggregate shape properties have on HMA performance.

DEDICATION

This thesis is dedicated to my mother Irene Flynt and father Doyle McGahan, who raised me to be the person I am today. The thesis is also dedicated to my sister Susan Hamm and brother Justin McGahan. I thank all of you for the endless love, support, and encouragement you have given me.

ACKNOWLEDGMENTS

First and foremost, I would like to thank Dr. Eyad Masad for giving me the opportunity to pursue my graduate studies here at Texas A&M University. He provided me with a great amount of encouragement and knowledge as he assisted me through my graduate studies. He is an amazing person whose passion for teaching and encouraging others will remain with me for many years. I would also like to thank Dr. Cliff Spiegelman from the Department of Statistics for helping me with the statistical analysis part of this research. Thanks are also due to Dr. Amy Epps-Martin for serving as a committee member and for her review of this thesis.

I would also like to thank the Federal Highway Administration (FHWA) for the funding they provided which allowed me to complete my graduate studies here at Texas A&M University. Thanks to Mr. Chuck Paugh and many others for providing me with performance data from the FHWA. Mr. Arif Chowdhury also provided a lot of help with the TTI projects I examined, as well as did Mr. Amit Bhasin.

I owe thanks to many of the students who helped me with this research. Thanks to Dr. Taleb Al-Rousan who aided me extremely in my initial months in graduate school. He basically introduced everything about the AIMS system to me. Thanks to Ms. Aparna Kanungo for her help on the AIMS software analysis. I would also like to thank Ms. Manjula Bathina, Mr. Dennis Gatchalian, and Mr. Anthony Luce for their help with the image analysis in this research.

TABLE OF CONTENTS

CHAPTER Page

LIST OF TABLES

TABLE Page

LIST OF FIGURES

CHAPTER I

INTRODUCTION

PROBLEM STATEMENT

Aggregate shape characteristics are known to affect the performance of hot mix asphalt (HMA) pavements in several ways. The work of many researchers has proven that these characteristics affect stability, permanent deformation, durability, and fatigue response of asphalt mixes. However, to date there have been few comprehensive studies aimed at correlating aggregate shape properties to actual HMA performance measurements. Accurate measurement of aggregate shape properties is vital to improving the design and performance of HMA pavements. The limitations of the standard techniques employed in Superpave^{TM} in measuring aggregate shape properties have restricted researchers in relating HMA performance to aggregate shape. The recently developed Aggregate Imaging System (AIMS) has proven to accurately and efficiently measure these aggregate shape properties. AIMS is a sophisticated testing device which is capable of measuring aggregate shape properties for both fine and coarse aggregates. AIMS results have proven to be reproducible and repeatable in regard to operator use and have also proven to be sensitive to slight variations in shape characteristics within an aggregate sample (Bathina, 2005). AIMS was used in this research to measure shape properties of a variety of aggregates used in several HMA

This thesis follows the style of the *Journal of Materials in Civil Engineering.*

mixes. These properties were then correlated to performance characteristics measured on each respective mix.

OBJECTIVES OF THE STUDY

The primary objective of this research is to relate aggregate shape properties to HMA performance measurements. This objective was achieved through completing the following tasks:

- Using AIMS to measure the aggregate shape properties of form, angularity, and texture of aggregate samples used in the three different projects incorporated in this research.
- Compiling databases that include the performance, volumetric, and aggregate shape measurements for each project.
- Conducting statistical analysis using computer software (SPSS®) to relate HMA performance measurements to aggregate shape properties.
- Explaining the relationships between HMA performance measurements and the aggregate shape properties.

REPORT ORGANIZATION

This report is organized into the following six chapters:

- Chapter I provides an introduction to the problem statement of this research, followed by the objectives and a brief outline of the report.

- Chapter II presents a literature review on the influence of aggregate shape properties on HMA performance. This chapter also includes a section describing AIMS features.
- Chapter III discusses the experimental measurements of HMA properties. It describes the HMA performance and volumetric measurements evaluated in each of the three projects being examined as well as the aggregates used in each.
- Chapter IV includes a discussion of AIMS measurements and the significance of these measurements in describing aggregate characteristics.
- Chapter V discusses the statistical analysis methods used to relate the HMA performance measurements with the aggregate shape properties. It also provides a summary of the results and discusses the statistical correlations between the HMA performance measurements and the aggregate shape properties.
- Chapter VI includes both conclusions and recommendations.

CHAPTER II

LITERATURE REVIEW

INTRODUCTION

This literature review thoroughly discusses the significance of aggregate properties in influencing the performance of HMA pavements. HMA pavements are the most common type of roadway surface used in the United States today. Federal Highway Administration (FHWA) data indicate that more than 90 percent of all pavements in the United States contain some type of asphalt surface. Asphalt pavement construction accounts for $15 billion per year in expenditures, approximately one-sixth of total highway operation expenses (Superpave System, The, 2000).

The high cost of operations in this field justifies the need for in depth research on characterization of asphalt pavement materials and development of methods for predicting HMA pavement performance. The effect of aggregate properties on performance of HMA pavements is one of the key topics that needs to be understood in order to optimize selection of aggregates for different loading and environmental conditions. Although the effect of aggregate on HMA performance is known intuitively, there is a lack of direct correlation relating aggregate properties to actual HMA performance. However, many researchers have noted the effect of aggregate shape characteristics on laboratory HMA specimens which will be discussed throughout this chapter.

THE INFLUENCE OF AGGREGATE PROPERTIES ON HMA PERFORMANCE

Aggregate particles can be defined in terms of three independent shape properties: shape (or form), angularity, and surface texture (Barrett, 1980). These three aggregate shape properties fully characterize particles based on their geometry. The form property characterizes aggregate particles based on ratios of particle dimensions. The angularity property measurement describes particles based on the variations at the edges of particles. This measurement defines particles in a range from rounded to angular. The final property is surface texture. This property describes the surface roughness of a particle at a small scale, which is not influenced by changes in form or angularity. These three properties are independent of each other: an increase or decrease in one of these properties does not necessarily influence the other two properties (Al-Rousan, 2004). A schematic diagram illustrating the differences between these three aggregate shape properties is shown in Figure 2.1.

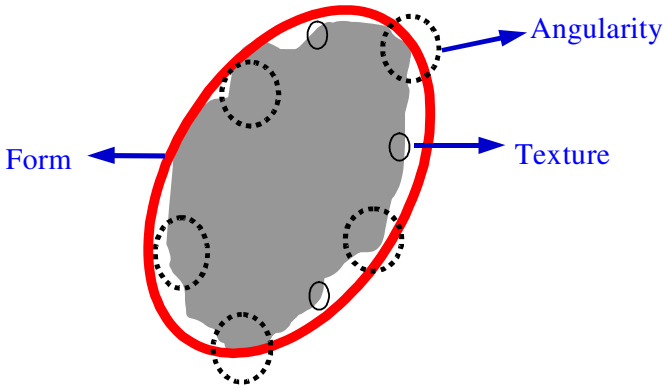

Fig. 2.1. Components of aggregate shape: form, angularity, and texture (Masad et al., 2003)

The current Superpave™ system does not use these three properties separately in describing aggregate shape, primarily because current methods used to characterize aggregate particles are not able to distinguish between different aggregate characteristics. In fact, recent studies have shown that the current method used in Superpave™ to measure fine aggregate angularity does not distinguish between poor and high quality aggregates (Huber et al., 1998; Chowdhury et al., 2001). Additionally, aggregate texture is not emphasized in the aggregate characterization methods currently used by Superpave™ (Fletcher et al., 2002). The current methods used in characterizing aggregate particles are not able to distinguish between the different shape properties. The development of a method capable of distinguishing between these characteristics, rather than a combination of their interactions, is vital in order to properly relate aggregate properties to HMA pavement performance (Masad et al., 2003).

The effects of aggregate shape and size on the stiffness and fatigue response of HMA mixes were examined by Monismith (1970). Monismith showed that stiffness and fatigue responses of HMA mixes are influenced by these aggregate characteristics. He recommended using rough-textured aggregates in a dense gradation to increase mix stiffness and fatigue life for thick HMA pavements. For thin pavements, Monismith recommended utilizing smooth-textured aggregates, which produce less stiff mixes and result in increased fatigue life (Monismith, 1970).

Foster (1970) compared the resistance of dense-graded HMA mixes containing both crushed and uncrushed coarse aggregates to traffic loads using pavement test sections. He concluded that HMA mixes containing crushed coarse aggregate perform

no better than mixes containing uncrushed coarse aggregate and that the true capacity of dense-graded mixes to resist traffic-induced stress is controlled by fine aggregate characteristics (Foster, 1970).

Lefebure (1957) used the Marshall test to measure the stability of HMA mixes containing either crushed cubical or crushed flat and elongated coarse particles. This research combined these two coarse aggregates with both natural and crushed fine aggregates. He concluded that fine aggregates provide the greatest influence on mix response (Lefebure, 1957).

Significant increases in Marshall stability were reported by Wedding and Gaynor (1961) when crushed gravel was substituted for uncrushed gravel in HMA mixes. The use of crushed coarse aggregates significantly increased HMA mix stability when compared to those that contained uncrushed gravel. The substitution of crushed coarse and fine aggregate for natural sand and gravel increased HMA stability by about 45 percent. They found that using crushed fine aggregates had minimal effect on HMA stability when crushed coarse aggregates were used. However, using crushed fine aggregates with uncrushed coarse aggregates resulted in a noticeable increase in HMA stability. They concluded that replacing natural sand with crushed gravel sand raises stability effectively equal to using 25 percent crushed gravel in the coarse aggregate (Wedding and Gaynor, 1961).

Moore and Welke (1979) tested Marshall stability on mixes that incorporated 110 different fine aggregates while keeping other components constant (coarse aggregate, asphalt content, mineral filler). They reported that fine aggregate angularity exhibits a

positive correlation with Marshall stability. An increase in aggregate angularity resulted in an increase in HMA mix stability (Moore and Welke, 1979).

Campen and Smith (1948) studied the influence of replacing natural round aggregates with crushed aggregates. Using Hubbard-Field and Bearing-Index tests, they reported a 30 to 190 percent increase in HMA mix stability when using crushed aggregates in dense-graded HMA mixes (Campen and Smith, 1948). Ishai and Gellber (1982) related HMA stability to geometric irregularities in aggregate particles using the packing volume concept developed by Tons and Goetz (1968). They found a significant increase in asphalt mix stability with increasing geometric irregularities of the aggregate particles (Ishai and Gelber, 1982). Kalcheff and Tunnicliff (1982) studied the effect of fine aggregate shape on HMA properties. Using the Marshall stability, repeated load triaxial compression, static indirect split-tensile, and repeated load indirect split-tensile tests, they found that replacing natural sand with manufactured sand improved the mix resistance to permanent deformation. Winford (1991) reached similar conclusions by comparing fine aggregate properties to mechanical properties of HMA.

Using triaxial compression testing methods, Herrin and Goetz (1954) studied the effect of aggregate shape on HMA mix stability. They reported that increasing the crushed gravel content in the coarse aggregate increases the strength of open-graded mixes; however, crushed gravel content had minimal effect on dense-graded HMA mixes (Herrin and Goetz, 1954). Field (1958) also studied the influence of crushed particles on HMA mixes. He found that HMA Marshall stability was not significantly affected when less than 35 percent of the coarse aggregates was crushed. HMA stability

increased consistently, however, as the percentage of crushed particles was raised to 100 percent. He reported average HMA stability 55 percent higher for 100 percent crushed particles when compared to mixes with 35 percent crushed particles (Field, 1958). Kandhal and Wenger (1973) also studied the effect of crushed coarse aggregate on dense-graded HMA mixes. Their research showed decreasing Marshall stability with increasing uncrushed coarse particle content in dense-graded HMA mixes.

Gaudette and Welke (1977) studied the effect of increasing the percent crushed faces of coarse aggregate particles in HMA mixes. Mixes containing between 0 and 50 percent crushed particles, regardless of the number of crushed faces, resulted in a stability increase of 17 percent over mixes without crushed particles. When more than 50 percent crushed particles was used, the stability of mixes containing particles with two or fewer crushed faces leveled off; however, the stability of mixes containing particles with three or more crushed faces continually increased with the percentage of crushed particles. Kandhal et al. (1991) performed an in depth analysis of factors that affect asphalt pavement performance. They found that HMA mixes containing less than 20 percent natural sand exhibited better overall performance than mixes containing more than 20 percent. For heavy-duty wearing and binder courses, the researchers recommended using coarse aggregates that contain more than 85 percent of particles with two or more fractured faces (Kandhal et al., 1991).

Sanders and Dukatz (1992) studied the effect of coarse aggregate angularity on permanent deformation using four HMA interstate pavement sections. After two years of operation, only one of the four sections exhibited permanent deformation. Upon

examination, they found that the HMA mix in the binder and surface coarse layers of the damaged section contained lower amounts of angular coarse aggregates than the undeformed sections (Sanders and Dukatz, 1992).

Maupin (1970) conducted a thorough laboratory investigation of the effect of particle shape on fatigue behavior of asphalt mixes. He used three aggregates: round gravel, crushed limestone, and slate. Using a constant strain mode fatigue test, Maupin (1970) concluded that mixes containing round gravel exhibited longer fatigue life than those containing crushed limestone or slate.

Li and Kett (1967) found that HMA mixes containing aggregates with a dimension ratio (longest to shortest dimensions) of less than 3:1 had no influence on Marshall or Hveem stability. They found the 30 to 40 percent particles with a dimension ratio larger than 3:1 did not adversely affect mix stability (Li and Kett, 1967). Kandhal and Parker (1998) also studied the influence of flat and elongated coarse aggregate particles on HMA strength and determined that excessive amounts of flat and elongated particles are undesirable in HMA mixes. Such particles were found to have a high tendency to fracture prior to application, which affected HMA mix durability (Kandhal and Parker, 1998).

Yeggoni et al. (1996) compared an imaging index of aggregate texture (fractal dimension) to creep behavior of asphalt mixes. Using the same gradation, seven different aggregate blends were prepared with varying amounts of crushed coarse aggregate particles. The relationship between the fractal dimension and the static creep compliance measured in this research can be seen in Figure 2.2.

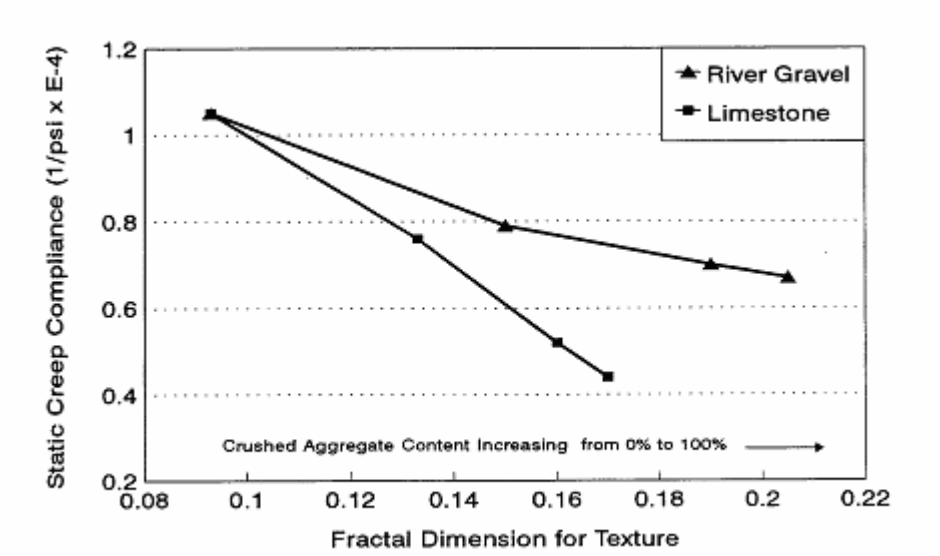

Fig. 2.2. Correlation between coarse aggregate texture measured using image analysis and rut depth in the creep compliance of HMA (Yeggoni et al., 1996)

Figure 2.3 compares the texture of the coarse aggregates used in the National Cooperative Highway Research Program (NCHRP) Project 4-19 (Kandhal and Parker, 1998) with rut depths of HMA pavements. The texture of these aggregates was measured using AIMS (Masad, 2003). The results show a distinct relationship between texture of coarse aggregates and resistance to permanent deformation.

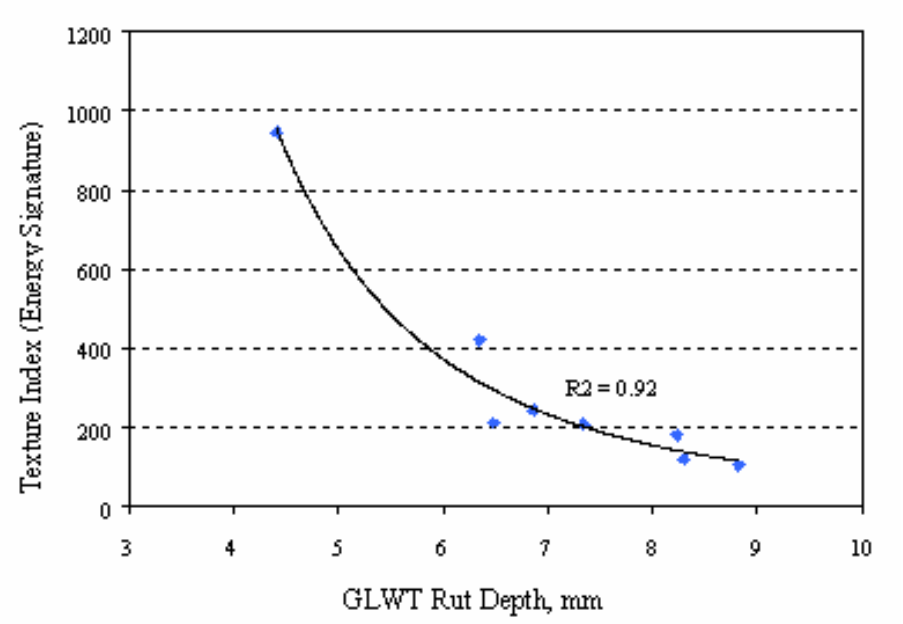

Fig. 2.3. Correlation between coarse aggregate texture measured using image analysis and HMA rut depth in the Georgia loaded wheel test (GLWT) (Fletcher et al., 2002)

THE AGGREGATE IMAGING SYSTEM (AIMS)

AIMS is a computer automated imaging system that measures aggregate shape properties. AIMS was developed by Dr. Eyad Masad through funding from the FHWA. Research performed by Dr. Taleb Al-Rousan led to development of a methodology for classifying aggregates based on their shape properties. Al-Rousan (2004) evaluated a large number of test methods for measuring aggregate shape and concluded that AIMS was the most effective system for measuring the shape characteristics of both fine and coarse aggregates. AIMS is capable of capturing all three distinct aggregate shape properties: form, angularity, and surface texture. Coarse aggregate particles are generally larger than 4.75 mm, and fine aggregate particles smaller than 4.75mm. AIMS

can analyze both coarse and fine aggregates, ranging from sizes of 150 μm to 37.5 mm (Masad, 2004).

AIMS has been evaluated through analysis of repeatability, reproducibility, and sensitivity in a recent study by Bathina (2005). She found that AIMS accurately measured the characteristics of both coarse and fine aggregates. Analysis showed that the maximum coefficient of variation (C.V.) of repeatability was 13.9 percent in measuring the texture of random samples and 4.9 percent in measuring the same sample several times by the same operator. Reproducibility analysis (variation among different operators) gave a maximum C.V. of 16.3 percent in measuring the texture of random samples. Bathina (2005) also concluded that AIMS is sensitive to changes in the distributions of form, angularity, and texture within an aggregate sample.

Bathina (2005) compared the repeatability and reproducibility results of AIMS to other test methods used to measure aggregate shape properties. She concluded that repeatability and reproducibility of AIMS measurements are excellent compared to other measurement methods.

CHAPTER III

EXPERIMENTAL MEASUREMENTS OF HMA PROPERTIES

INTRODUCTION

HMA mixes from three separate projects were used in this research to investigate the relationship between aggregate characteristics, mix volumetrics, and performance. The previous projects were conducted at Texas Transportation Institute (TTI) and at FHWA's mobile laboratory. The tests involved measuring volumetric and mechanical properties of a variety of HMA mixes with different aggregate sources and binder grades. This chapter describes these mixes and their properties.

FHWA MOBILE LABORATORY PROJECTS

The mixes in this section were collected and tested at FHWA's mobile laboratory. This mobile laboratory travels across the Unites States testing HMA mixes used in different pavements. The FHWA has compiled a database for tested mixes that includes performance parameters and volumetric measurements. Some state specifications for mix volumetrics differ. These criteria are influenced by the environmental surroundings of the pavements as well as the state or local design codes for each location.

Extensive evaluation was conducted on the FHWA database in order to compile the same volumetrics, performance measurements, and aggregate shape properties for the mixes included in this research. Some of the pavements examined in the FHWA

mobile laboratory unit did not record some of the volumetric measurements and had to be excluded from the project. For instance, the Florida mixes were removed because binder shear modulus (G*) was not measured. Table 3.1 lists the sources of the mixes used in this research.

Aggregates and HMA Volumetrics

The FHWA provided samples of the aggregates used in each mix so that the aggregate properties could be measured using AIMS. They conducted sieve analyses on the aggregates used in the mixes, and these aggregate gradations are shown below in Table 3.1.

Table 3.1. FHWA Mobile Laboratory Aggregate Sieve Data

Sieve Size (mm)	Percent Passing							
	Wiscon-sin	Iowa	Maine	North Carolina	Minne-sota	Kansas	Wash-ington	Louis-iana
25.00	100.0	100.0	100.0	100.0	100.0	100.0	100.0	97.5
19.00	98.1	99.9	100.0	100.0	100.0	97.9	100.0	88.4
12.50	88.4	93.5	100.0	99.6	94.0	89.2	95.7	70.0
9.50	78.5	86.6	97.9	93.9	87.5	84.9	85.3	55.0
4.75	62.4	60.7	61.8	65.6	66.9	65.9	54.1	32.6
2.36	42.5	40.4	38.1	52.8	47.8	41.1	32.5	24.1
1.18	27.2	29.3	24.7	44.7	32.6	26.6	20.9	19.3
0.60	17.0	22.2	16.4	31.1	22.0	17.1	14.7	15.5
0.30	9.1	13.9	10.7	16.8	12.9	9.3	10.8	7.8
0.15	5.7	8.2	8.0	9.2	6.8	5.3	8.3	4.4
0.08	4.7	5.2	6.1	5.7	3.8	3.9	6.5	3.3

The HMA volumetrics and binder properties measured in this project can be seen in Table 3.2. The first volumetric parameter measured is voids in mineral aggregate (VMA), which is a measurement of the total voids within a compacted aggregate. VMA, along with many of the other volumetrics listed in Table 3.2, is known to affect the performance of HMA mixes. If VMA is too low the mix will have a low film thickness, resulting in low durability. Conversely, if VMA is too high, the mix will have a high film thickness leading to stability problems in the mix (Roberts et al., 1996). The second volumetric parameter is voids filled with asphalt (VFA), which is a measurement of the percentage of voids in the mix that are filled with asphalt. This volumetric property also affects HMA mix stability and is generally limited to a range of 70 to 85 percent (Roberts et al., 1996).

Table 3.2. FHWA Mobile Laboratory Mix Volumetric and Binder Properties

Mix Volumetric and Binder Properties
Voids in Mineral Aggregate (VMA)
Voids Filled with Asphalt (VFA)
Design Voids in Total Mix (VTM)
VTM when Tested
Asphalt Content
High PG Temperature
G* (Binder Shear Modulus)
Temperature at G* Measurement
Performance Parameters Measurement Temperature

The next parameter is the design voids in the total mix (VTM). This measurement is probably the most important factor that affects mix performance

throughout the life of HMA pavements (Roberts et al., 1996). In Superpave™, asphalt mixes are designed to attain 4 percent VTM at the design number of gyrations. The actual VTM (when tested) in the mix is the next volumetric parameter. The fifth volumetric parameter is the asphalt content. This value is the percent of asphalt by weight of the mix. The optimum design asphalt content is determined from compaction and volumetric data.

Every asphalt sample is designated through the Superpave™ grading system with a high and low performance grade (PG) temperature. These temperatures are used to correlate performance with binder properties. Binder dynamic shear modulus (G*) was measured at a frequency of 10 radians/sec at the maximum grading temperature. The temperature at which the performance parameters were measured is also included as an independent parameter in the regression analysis. The results of HMA property measurements can be seen in Table 3.3. The numbers given in the first column of Table 3.3, where included, refer to the percent asphalt content in the mix.

Table 3.3. FHWA Mobile Laboratory Mix Volumetric and Binder Properties Data

State	Mix Volumetric and Binder Properties								
	VMA (%)	**VFA (%)**	**Design VTM (%)**	**VTM when Tested (%)**	**Asphalt Content (%)**	**G* (KPa)**	**High PG Temp. (°C)**	**Temp. G* was Measured (°C)**	**PPMT (°C)**
Wisconsin Mix Rep.	15.1	72.4	4.0	8.0	5.5	1.44	64	64	31
Wisconsin Plant	14.8	67.7	4.8	8.0	4.7	1.44	64	64	31
Iowa Mix Rep.	14.8	68.2	4.7	6.0	5.4	1.19	58	58	40
Iowa Plant	13.0	76.2	4.7	6.0	5.5	1.19	58	58	40
Maine Mix Rep.	14.3	68.5	4.5	5.0	5.8	1.28	64	64	38
Maine Plant	14.7	69.8	4.5	5.0	6.1	1.28	64	64	38
N.C. Mix Rep.	12.0	79.4	2.5	8.0	5.0	1.23	70	70	45
N.C. Plant	13.0	72.1	3.6	8.0	5.0	1.23	70	70	45
Louisiana 3.3	12.4	55.6	5.5	7.5	3.3	1.96	64	64	54
Louisiana 3.8	12.5	65.6	4.3	7.5	3.8	1.96	64	64	54
Louisiana 4.3	12.3	77.2	2.8	7.5	4.3	1.96	64	64	54
Louisiana Plant	12.4	63.7	4.5	7.5	3.8	1.96	64	64	54
Washington 5.5	14.5	69.0	4.5	8.0	5.5	1.34	64	64	45
Washington 6	14.7	75.5	3.6	8.0	6.0	1.34	64	64	45
Washington 6.5	14.3	86.7	1.9	8.0	6.5	1.34	64	64	45
Washington Plant	14.7	75.5	3.6	7.7	6.0	1.34	64	64	45
California Hveem w/ Rap	10.8	86.1	1.5	8.3	4.8	1.29	64	64	48
California Hveem w/o Rap	10.7	69.2	3.3	7.9	4.6	1.29	64	64	45
California Superpave™	13.4	74.6	3.4	8.1	5.2	1.29	64	64	45
Kansas 4.7	15.1	56.3	6.6	6.9	4.7	1.42	64	64	45
Kansas 5.2	14.8	64.2	5.3	7.0	5.2	1.42	64	64	45
Kansas 5.7	14.8	74.3	3.8	7.1	5.7	1.42	64	64	45
Kansas Plant	14.3	65.7	4.9	7.1	5.2	1.42	64	64	45
Minnesota 4.8	16.8	56.0	7.4	8.0	4.8	1.15	70	70	45
Minnesota 5.3	15.6	68.6	4.9	8.0	5.3	1.15	70	70	45
Minnesota 5.8	16.2	73.5	4.3	8.0	5.8	1.15	70	70	45
Minnesota Plant	15.4	69.5	4.7	8.0	5.3	1.2	70	70	45

Notes: Rap denotes recycled asphalt pavement. PPMT labels the performance parameters measurement temperature quantity.

Table 3.4. FHWA Mobile Laboratory Mix Performance Parameters

Performance Parameters
Flow Point
Strain @ Flow
Total Accumulated Strain
N Failure
Flow Slope
Flow to Termination Slope

HMA Performance Parameters

The performance parameters measured at the FHWA mobile laboratory are shown in Table 3.4. The first performance parameter, flow point, is the number of cycles an asphalt specimen can withstand before it reveals an increasing rate of shear deformation development in a dynamic creep test. Figure 3.1 below shows an illustration of strain response of an asphalt sample when a cyclic load is applied to the specimen. The flow point is easily identifiable on the graph. It is located where the graph changes concavity, also known as an inflection point. This occurs in Figure 3.1 at a value of 5,000 cycles and is denoted at point A.

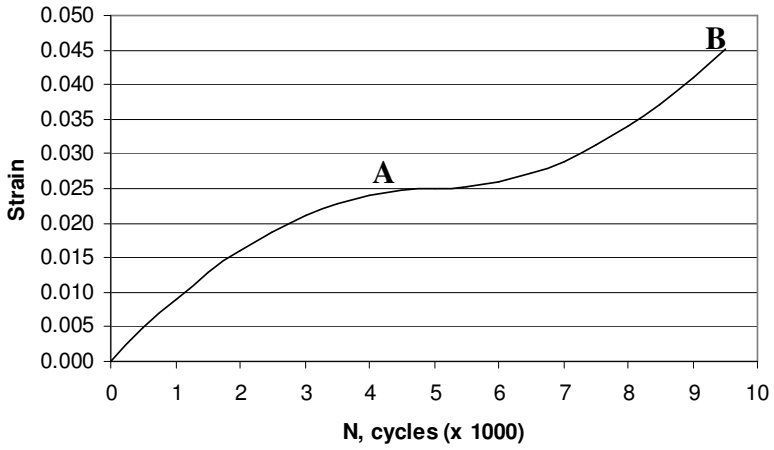

Fig. 3.1. Illustration of flow test results

The second performance parameter is strain @ flow, which is also shown in Figure 3.1 at point A at a strain of 0.025. The third and fourth performance parameters are also derived from the flow test. The total accumulated strain is the maximum strain the sample reaches before it fails. In Figure 3.1 above, this maximum value is reached when the asphalt specimen fails and is labeled by point B. However, some asphalt samples exhibit a reduction in strain as the sample approaches failure. The fourth performance parameter is the number of cycles the asphalt specimen withstands before failure. This occurs in Figure 3.1 at around 9,500 cycles and is labeled by point B at a total accumulated strain of 0.045.

The final two performance parameters are arithmetic functions that combine the previous performance parameters. Both of these functions use the logarithmic components of each parameter to linearize the flow graph data. The first function is labeled as the Flow Slope and incorporates the Strain @ Flow and Flow Point performance parameters. The second function, Flow to Termination Slope, incorporates the Total Strain, Strain @ Flow, N Failure, and Flow Point performance parameters. The equations for these two performance parameters can be seen in Equations 1 and 2. The performance measurement data for these FHWA mixes are shown in Table 3.5.

$$\text{Flow Slope} = \frac{\log \text{ Strain @ Flow}}{\log \text{ Flow Point}} \quad (1)$$

$$\text{Flow to Termination Slope} = \frac{\log \text{ Total Strain - log Strain @ Flow}}{\log \text{ N Failure - log Flow Point}} \quad (2)$$

Table 3.5. FHWA Mobile Laboratory Performance Measurement Data

Mix Source	Type of Mix Design	PPMT (°C)	Flow Point, (cycles)	Strain @ Flow	Total Accumulated Strain	Total Cycles
Wisconsin	Mix Replication	31.2	7,655.0	8,529.4	12,283.8	10,701.9
	Plant Produced	31.2	4,392.7	13,514.6	28,812.5	8,803.4
Iowa	Mix Replication	40.0	376.0	14,407.8	50,134.9	1,263.3
	Plant Produced	40.0	309.8	15,084.8	50,095.2	932.0
Maine	Mix Replication	37.5	4,002.0	14,515.0	30,258.0	9,316.0
	Plant Produced	37.5	2,093.0	19,670.0	46,405.0	5,778.0
North Carolina	Mix Replication	45.0	777.6	22,306.0	50,026.0	2,251.0
	Plant Produced	45.0	496.0	16,900.0	50,038.0	1,554.0
Louisiana	3.3 Mix	54.0	141.0	25,374.0	50,143.0	360.0
	3.8 Mix	54.0	141.0	28,812.0	50,123.0	328.0
	4.3 Mix	54.0	96.0	40,083.8	50,112.0	185.5
	Plant Produced	54.0	222.6	28,182.5	50,136.8	541.6
Washington	5.5 Mix	45.0	373.0	23,179.0	50,034.0	1,028.0
	6 Mix	45.0	239.0	30,429.0	50,052.0	512.0
	6.5 Mix	45.0	156.0	34,473.0	50,081.0	319.0
	Plant Produced	45.0	261.0	25,513.7	50,051.3	653.5
California	Hveem w/ Rap	48.4	336.0	34,584.0	50,034.0	634.0
	Hveem w/o Rap	45.0	215.0	26,146.0	50,073.0	542.0
	Superpave™	45.0	906.0	25,336.0	50,014.0	2,159.0
Kansas	4.7 Mix	45.0	151.0	20,113.0	50,202.0	436.0
	5.2 Mix	45.0	141.0	20,664.0	50,170.0	392.0
	5.7 Mix	45.0	96.0	34,986.0	50,243.0	191.0
	Plant Produced	45.0	157.3	23,495.5	50,133.9	422.9
Minnesota	4.5 Mix	45.0	282.8	18,478.3	50,104.3	847.0
	5.3 Mix	45.0	220.0	20,986.9	50,119.1	634.9
	5.8 Mix	45.0	261.0	19,288.0	50,084.8	802.5
	Plant Produced	45.0	433.9	20,044.8	50,052.0	1,283.8

TTI PROJECT 9-558

The second set of data examined was generated during TTI Project 9-558. This project, titled "Evaluation of Simple Performance Tests on HMA Mixtures in the South Central USA," was completed in April 2003 in cooperation with the Texas Department of Transportation (TxDOT) and FHWA. Project 9-558 examined a wide variety of asphalt materials and mix designs used in the south central region of the United States (nine sections) in addition to three laboratory designed mixes (Bhasin et al., 2003).

Aggregates and HMA Volumetrics

The aggregates from this project were retrieved from the TTI's laboratory where they were originally used in TTI Project 9-558. This research evaluated 12 mixes; however, only 10 of these mixes were incorporated into this research because the aggregates and mix properties from the other two could not be obtained. Table 3.6 shows the sieve analyses results for the mixes used in this research. The volumetric measurements shown in Table 3.7 were taken from TTI Report 9-558 (Bhasin et al., 2003). These volumetrics are the same as those measured in the FHWA mixes discussed in the previous section.

Table 3.6. Project 9-558 Aggregate Sieve Data (Bhasin et al., 2003)

Sieve Size (mm)	Percent Passing									
	ARTL	ARLR	LA	NM Bingham	NM Vado	OK	TX WF	TX Bryan	64-40 RG	64-40 RHY
37.50	100.0	100.0	100.0	100.0	100.0	100.0	100.0	100.0	100.0	100.0
25.00	100.0	100.0	100.0	100.0	100.0	100.0	100.0	100.0	100.0	100.0
19.00	100.0	100.0	100.0	100.0	99.0	100.0	100.0	100.0	100.0	100.0
12.50	100.0	100.0	95.3	93.0	77.0	96.0	97.1	100.0	100.0	100.0
9.50	92.0	94.0	83.0	82.0	66.0	81.0	79.3	66.9	93.7	100.0
4.75	56.0	62.0	62.3	59.0	44.0	54.0	45.9	34.1	70.7	99.5
2.36	39.0	46.0	43.7	41.0	26.0	38.0	30.7	18.8	41.6	88.1
1.18	28.0	31.0	31.5	28.0	19.0	25.0	19.5	11.0	26.7	54.7
0.60	23.0	21.0	22.9	19.0	14.0	17.0	11.8	8.7	18.1	22.7
0.30	15.0	11.0	12.4	12.7	10.0	13.0	6.8	7.2	11.1	9.8
0.15	7.0	7.0	6.9	9.2	7.2	9.0	3.9	0.0	4.6	8.0
0.08	5.1	4.4	5.1	5.8	5.8	5.8	3.2	0.0	2.9	6.1

Notes: Mixes 3 and 10 from project 9-558 were not included due to the unavailability of aggregates or mix properties.

Table 3.7. Project 9-558 Mix Volumetric and Binder Properties Data

Aggregate Source		Mix Volumetric and Binder Properties				
Aggregate Reference #	Aggregate Reference	VMA (%)	VFA (%)	Design VTM (%)	Asphalt Content (%)	High PG Temperature (°C)
1	ARTL	16.5	72.5	4.5	6.0	64
2	ARLR	15.8	71.8	4.5	5.8	64
4	LA	14.8	73.0	4.0	4.7	70
5	NM Bingham	14.0	71.3	4.0	4.3	70
6	NM Vado	14.6	72.8	4.0	4.8	82
7	OK	15.2	73.0	4.0	4.8	70
8	TX WF	15.3	73.7	4.0	4.8	76
9	TX Bryan	14.0	75.0	3.5	4.5	64
11	64-40 RG	16.3	75.4	4.0	5.5	64
12	64-40 RHY	14.1	75.1	3.5	7.8	64

HMA Performance Parameters

The performance parameters used in Project 9-558 are listed in Table 3.8. The first performance parameter examined in this research was creep compliance, which is the ratio of measured strain to applied constant stress on an asphalt sample. The second parameter is strain @ flow. This performance measurement was discussed in the previous section.

Table 3.8. Project 9-558 Performance Measurement Data

Aggregate Data		**Measured Performance Parameters**				
Aggregate Reference #	**Aggregate Reference**	**Compliance (1/MPa)**	**Strain @ Flow**	**E*/sin ϕ at 10 Hz (Avg. 1000 MPa)**	**APA Rut Depth (in)**	**Flow Point (cycles)**
1	ARTL	0.17	0.28	2.1	8.2	0.2
2	ARLR	0.03	0.17	0.8	18.9	0.2
4	LA	0.06	0.07	1.4	7.2	0.4
5	NM Bingham	0.01	0.01	4.4	2.5	15
6	NM Vado	0.01	0.004	5	2	15
7	OK	0.08	0.08	1	4.2	3.6
8	TX WF	0.035	0.04	2.7	3.6	3.2
9	TX Bryan	0.02	0.02	2.5	4.7	5.8
11	64-40 RG	0.295	0.27	0.8	6.3	0.2
12	64-40 RHY	0.335	0.31	1.5	3.8	1.6

The next performance parameter is E*/sin ϕ at a frequency of 10 Hz. This value incorporates the dynamic modulus E* and the phase angle ϕ. Dynamic modulus is the ratio of amplitude stress to amplitude strain measured under cyclic loading. The phase angle Φ provides an indication of the proportions of the viscous and elastic behavior of the asphalt binder. A purely elastic material has a Φ value of 0^o, while a purely viscous material has a Φ value of 90^o.

The next parameter is rut depth (in millimeters) measured in the asphalt paving analyzer (APA). The APA is a laboratory wheel testing device in which an asphalt mix slab or a cylindrical specimen is subjected to wheel passes to induce rutting (Bhasin et al., 2003). This performance parameter predicts the rutting susceptibility of an asphalt pavement after a predetermined number of passes are applied to each asphalt sample.

The final performance parameter is flow point. This parameter, previously discussed in the FHWA mobile laboratory project, is the number of cycles an asphalt sample can withstand before revealing an increasing rate of permanent deformation in a dynamic creep test.

Figure 3.2 depicts the typical relationship between total cumulative permanent deformation and the number of loading cycles in a dynamic creep test. In this type of test, Kaloush and Witczak (2002) described three zones on a permanent strain versus loading repetitions graph: a primary zone, a secondary zone, and a tertiary zone. The primary zone, as shown in Figure 3.2, is the initial area of the curve before the relationship becomes linear. The secondary zone, located in the center of the figure, exhibits a linear relationship between permanent strain and loading repetitions. The tertiary zone begins when the curve shows positive acceleration after the linear behavior ceases. The flow point is located at the point where the tertiary zone begins. This is where the rate of change of compliance is at the minimum (Kaloush and Witczak, 2002).

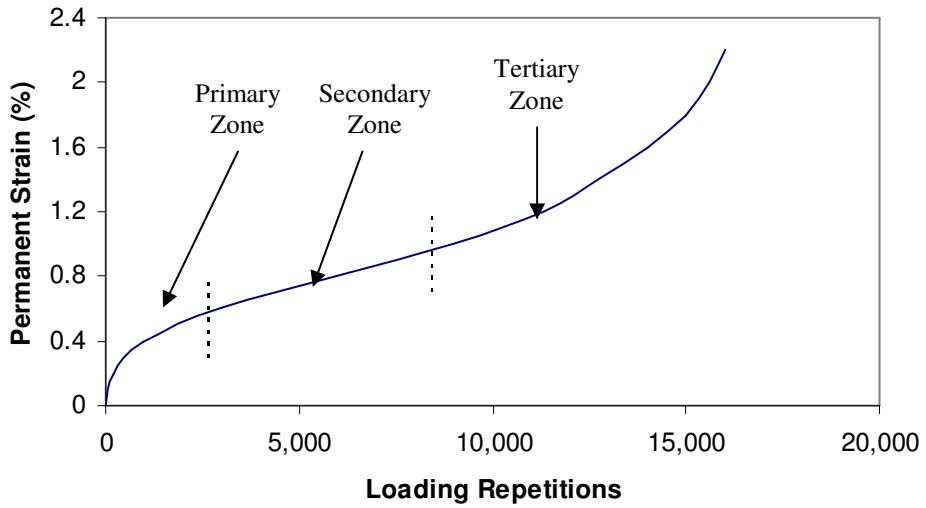

Fig. 3.2. Dynamic creep test expressing the primary, secondary, and tertiary zones

TTI PROJECT 4203

The third and final project incorporated in this research was from a project conducted at TTI. This TTI project, in cooperation with FHWA and TxDOT, was completed in March 2003 as part of the Cooperative Research Program: "As-Built Properties of Test Pavements on IH-20 in Atlanta District." This project involved the construction of nine HMA test sections on IH-20 in Harrison County. These sections were constructed using different mix designs: three primary aggregate types and three mix design types. All mixes used the same asphalt (PG 76-22) source (Chowdhury et al., 2003).

Aggregates and HMA Volumetrics

The three primary types of aggregates used in this project were quartzite, sandstone, and siliceous river gravel. Table 3.9 lists the sources and suppliers of the primary aggregates used in this project. Each primary type of aggregate was used in the three designs, also shown in Table 3.9.

Table 3.9. Project 4203 Aggregate Types and Mixes (Chowdhury et al., 2003)

Aggregate Type	Aggregate Supplier	Aggregate Source	Test Section Number		
			Superpave™	CMHB-C	Type C
Quartzite	Martin Marietta	Jones Mill	#3	#6	#9
Sandstone	Meridian	Sawyer, OK	#2	#5	#8
Siliceous River Gravel	Hanson	Prescott, AK	#1	#4	#7

Table 3.10 shows the aggregates used in each mix design. Each mix design incorporated hydrated lime and supplementary aggregates to serve as intermediate/fine aggregates. These additional aggregates and their percentages are shown in Table 3.10.

Table 3.10. Project 4203 Aggregate Mix Designs

Design Type	Test Section #	Aggregate Mix Designs	
		Percent Used	**Aggregate Type**
Superpave™	#1	67	Siliceous River Gravel
		32	Limestone Screenings
		1	Hydrated Lime
	#2	91	Sandstone
		8	Igneous Screenings
		1	Hydrated Lime
	#3	89	Quartzite
		10	Igneous Screenings
		1	Hydrated Lime
CMHB-C	#4	79	Siliceous River Gravel
		20	Igneous Screenings
		1	Hydrated Lime
	#5	87	Sandstone
		12	Igneous Screenings
		1	Hydrated Lime
	#6	87	Quartzite
		12	Igneous Screenings
		1	Hydrated Lime
Type C	#7	61	Siliceous River Gravel
		30	Limestone Screenings
		8	Igneous Screenings
		1	Hydrated Lime
	#8	99	Sandstone
		1	Hydrated Lime
	#9	91	Quartzite
		8	Igneous Screenings
		1	Hydrated Lime

The three Superpave™ mixes were designed to address 30 million equivalent single axle loads (ESALs). On the gyratory compactor, the N_{ini}, N_{des}, and N_{max} were set to 9, 125, and 205, respectively. The Superpave™ design followed Tex-204-F Part IV procedure (Chowdhury et al., 2003). The aggregate gradation and mix design summary for the Superpave™ mixes can be seen in Tables 3.11 and 3.12.

Table 3.11. Aggregate Gradation for Superpave™ Mixes Used in Project 4203 (Chowdhury et al., 2003)

Sieve Size (mm)	**Cumulative Percent Passing**		
	Siliceous River Gravel (Section #1)	Sandstone (Section #2)	Quartzite (Section #3)
19.00	100.0	100.0	100.0
12.50	92.0	92.1	93.7
9.50	84.8	79.4	81.7
4.75	52.4	49.0	45.5
2.36	30.9	29.2	31.4
1.18	20.4	22.4	21.0
0.60	13.9	18.9	17.7
0.30	8.8	14.9	11.8
0.15	4.5	10.2	8.2
0.08	3.2	6.5	5.6

Table 3.12. Project 4203 Superpave™ Mix Design Summary (Chowdhury et al., 2003)

Mix	**Optimum Asphalt Content (%)**	**Design Air Void (%)**	**VMA (%)**	**VFA (%)**	**Percent G_{mm} at N_{ini}**	**Percent G_{mm} at N_{max}**	**Dust Pro-portion**
Siliceous River Gravel (Section #1)	5.0	3.7	15.3	73.9	86.9	97.5	0.6
Sandstone (Section #2)	5.1	3.8	15.1	73.1	86.0	97.4	1.3
Quartzite (Section #3)	5.1	3.8	15.6	73.1	86.5	97.4	1.1
Specifications	N/A	4.0±1.0	14.0 Min	65-75	89.0 Max	98.0 Max	0.6-1.2

The three CMHB-C mixes followed the TxDOT mix design procedure Tex-294-F Part II (Chowdhury et al., 2003). The aggregate gradation and mix design summary for these mixes can be seen in Tables 3.13 and 3.14.

Table 3.13. Aggregate Gradation for CMHB-C Mixes Used in Project 4203 (Chowdhury et al., 2003)

Sieve Size (in)	**Cumulative Percent Passing**		
	Siliceous River Gravel (Section # 4)	Sandstone (Section # 5)	Quartzite (Section #6)
7/8	100.0	100.0	100.0
5/8	99.7	100.0	99.6
3/8	64.5	65.4	65.6
#4	34.3	38.0	34.2
#10	21.8	24.0	24.0
#40	16.2	16.4	14.5
#80	9.8	10.9	9.1
#200	6.4	6.4	5.9

Table 3.14. Project 4203 CMHB-C Mix Design Summary (Chowdhury et al., 2003)

Mix	**Optimum Asphalt Content %**	**Design Air Void %**	**VMA %**
Siliceous River Gravel (Section #4)	4.7	3.5	14.1
Sandstone (Section #5)	4.8	3.5	14.6
Quartzite (Section #6)	4.8	3.5	14.1

The three Type C mixes followed the TxDOT mix design procedure Tex-294-F Part I (Chowdhury et al., 2003). The aggregate gradation and mix design summary for the Type C mixes are shown in Tables 3.15 and 3.16.

Table 3.15. Aggregate Gradation for Type C Mixes Used in Project 4203 (Chowdhury et al., 2003)

Sieve Size (in)	**Cumulative Percent Passing**		
	Siliceous River Gravel (Section #7)	Sandstone (Section #8)	Quartzite (Section #9)
7/8	100.0	100.0	100.0
5/8	100.0	99.8	99.8
3/8	75.8	80.7	79.1
#4	49.2	46.2	51.4
#10	31.5	30.9	34.0
#40	18.2	15.6	17.9
#80	11.7	9.6	10.0
#200	5.8	5.8	5.3

Table 3.16. Project 4203 Type C Mix Design Summary (Chowdhury et al., 2003)

Mix	**Optimum Asphalt Content (%)**	**Design Air Void (%)**	**VMA (%)**
Siliceous River Gravel (Section #7)	4.4	4.0	14.0
Sandstone (Section # 8)	4.5	4.0	14.1
Quartzite (Section #9)	4.6	4.0	14.6

The base material used under all the pavements in this project was created using approximately 90 percent limestone aggregate and 10 percent field sand. The limestone was obtained from Hanson (Perch Hill), and the field sand was collected in Marshall,

Texas. Table 3.17 gives the mix design data and gradation of the base material used in this project (Chowdhury et al., 2003). The mix volumetric and binder properties data for this project are shown in Table 3.18. All of these volumetric parameters were previously defined in the FHWA mobile laboratory project.

Table 3.17. Base Mix Design Summary for Project 4203 (Chowdhury et al., 2003)

Sieve Size (in)	**Percent Passing**	**Design Summary**	
7/8	100.0	Optimum Asphalt Content (%)	3.8
5/8	90.1		
3/8	79.4	Design Air Void (%)	4.0
#4	52.9		
#10	31.9	Design VMA (%)	13.0
#40	19.4		
#80	9.8	Rice Specific Gravity (gm/cc)	2.516
#200	3.8		

Table 3.18. Project 4203 Mix Volumetric and Binder Properties Data

Aggregate Type	**Mix #**	**Mix Volumetric and Binder Properties**						
		VMA (%)	**VFA (%)**	**Design VTM (%)**	**VTM when Tested (%)**	**Asphalt Content (%)**	**High PG Temp. (°C)**	**Performance Test Temp. (°C)**
Quartzite	3	15.6	73.1	3.8	6.8	5.1	76	64
	6	14.1	74.0	3.5	6.7	4.8	76	70
	9	14.6	72.9	4.0	7.2	4.6	76	64
Sandstone	2	15.1	73.1	3.8	6.7	5.1	76	70
	5	14.6	76.3	3.5	5.8	4.8	76	70
	8	14.1	71.4	4.0	6.4	4.5	76	82
River Gravel	1	15.3	73.9	3.7	7.1	5.0	76	70
	4	14.1	76.8	3.5	6.5	4.7	76	64
	7	14	73.8	4.0	7.1	4.4	76	76

HMA Performance Parameters

Table 3.19 gives the HMA performance measurements data. The first performance parameter is average E* measured at 5 Hz. This value, known as dynamic modulus, is a measure of an HMA specimen's stress/strain response to axial loading. In this project, the dynamic modulus was measured at four different temperatures: 40°F, 70°F, 100°F, and 130°F.

Table 3.19. Project 4203 Performance Measurement Data

Aggregate Type	Mix #	Measured Performance Parameters						
		Avg E* (x10^3 psi) @ 5 Hz				Hamburg Deformation (in)	APA Rut Depth (in)	Average IDT Strength (psi)
		40° F	70° F	100° F	130° F			
Quartzite	3	1,869	1,136	336	87	0.0	0.1	154.2
	6	1,874	1,118	394	143	0.1	0.2	159.1
	9	2,130	1,025	283	106	0.1	0.1	176.1
Sandstone	2	2,736	1,553	454	168	0.1	0.2	226.4
	5	2,415	1,255	373	118	0.1	0.2	205.2
	8	2,936	1,543	563	139	0.1	0.1	213.7
River Gravel	1	2,217	1,213	400	136	0.1	0.1	174.0
	4	2,047	1,008	317	102	0.1	0.2	168.9
	7	2,433	1,265	390	117	0.1	0.1	173.6

The second performance parameter is Hamburg Deformation. The Hamburg test is used to express an HMA sample's response to permanent deformation. The Hamburg wheel was constrained to 20,000 passes in the test to serve as a common measurement point.

The next performance parameter listed is APA Rut Depth. This test, also used in TTI Project 9-558, is used to determine the rutting susceptibility of asphalt pavements. The fourth performance parameter is average IDT strength. The Indirect Tension Test, commonly known as IDT, measures the tensile capacity of an HMA sample by applying a compression load on a cylindrical sample across its diameter. It is used to simulate how HMA responds to tensile forces. The IDT test was performed according to the Tex-226-F procedure (Chowdhury et al., 2003).

CHAPTER IV

AGGREGATE SHAPE PROPERTIES

INTRODUCTION

Aggregate shape is a term used to characterize and classify aggregates based on three distinct geometric properties: form, angularity, and surface texture. These properties can be measured by several methods. Geologists have traditionally used visual charts to classify aggregates based on their shape characteristics. Figures 4.1 and 4.2 show the classification charts used by geologists for ranking aggregate angularity and form, respectively. Using these visual charts is far less accurate and more time consuming than many modern methods used today. AIMS was used in this research to classify and measure aggregate shape. This chapter describes the main AIMS components and the types of measurements that AIMS records.

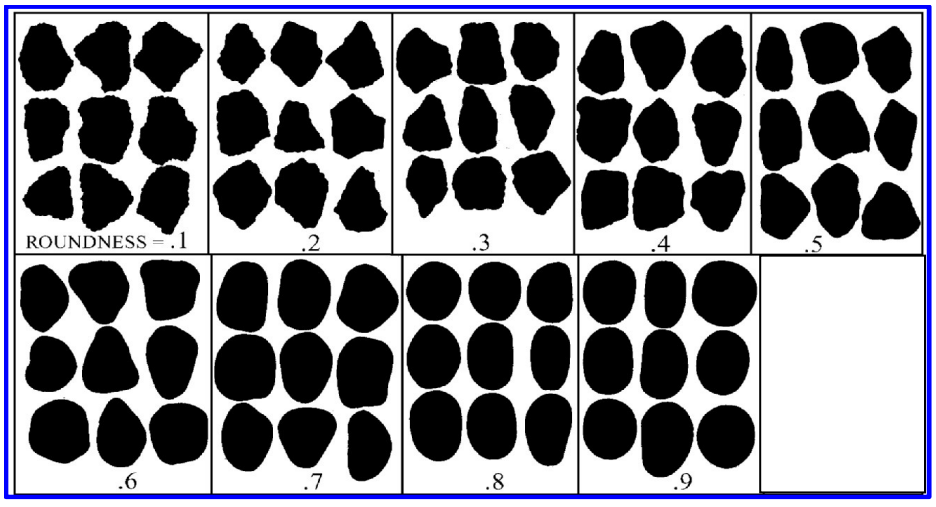

Fig. 4.1. Angularity classification chart (Krumbein, 1941)

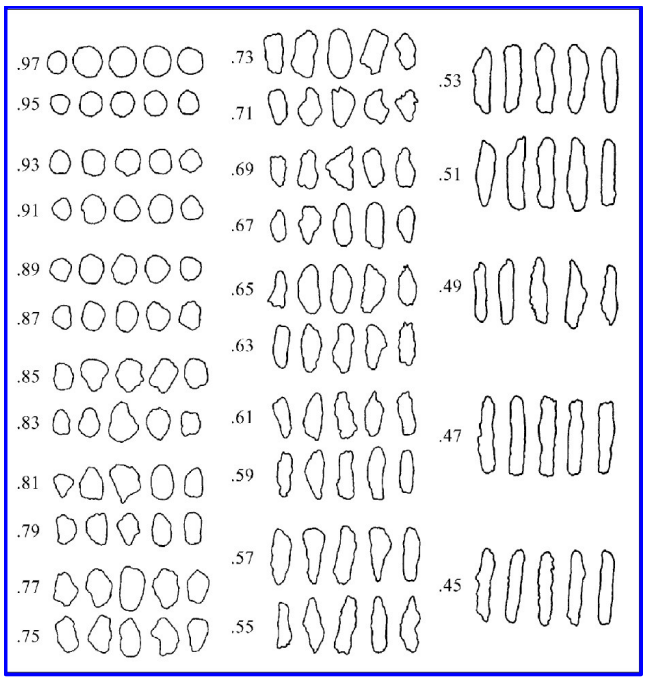

Fig. 4.2. Form classification chart (Rittenhouse, 1943)

CAPABILITIES OF AIMS

AIMS is a highly sophisticated system that accurately and efficiently measures the aggregate shape properties of form, angularity, and surface texture. Figure 4.3 shows the AIMS system.

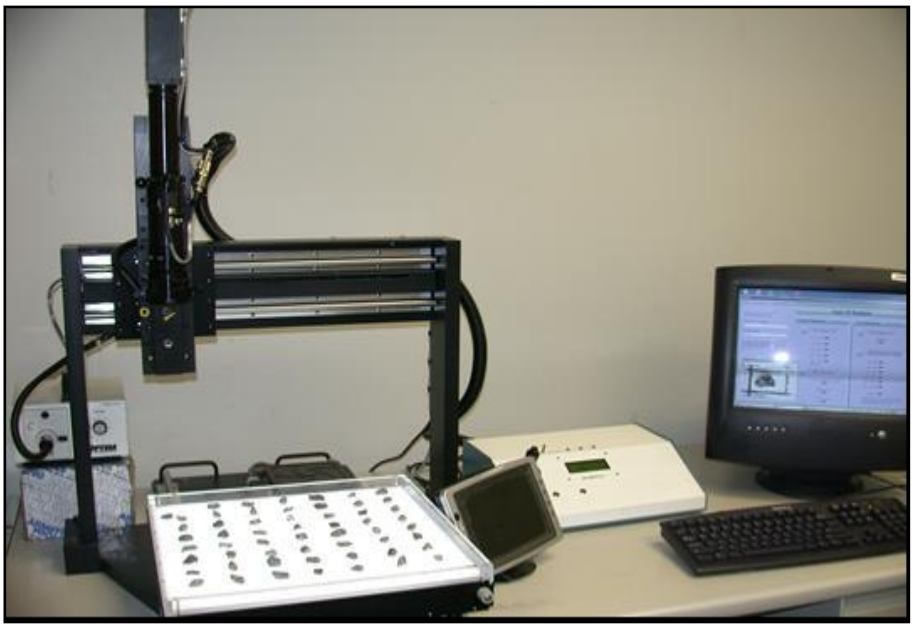

Fig. 4.3. Illustration of AIMS setup (Al-Rousan, 2004)

The system operates in conjunction with a computer, which is shown in the right of Figure 4.3. The object on the left-hand side is the AIMS hardware, which performs the aggregate scanning. The aggregate test sample is placed on the white tray shown in the bottom left of Figure 4.3. Coarse aggregate particles are placed on preset grid point locations, while fine aggregates are randomly spread over the tray. The system contains a camera unit that uses an Optem zoom 160 video microscope. The system is equipped with tube lighting from the microscope unit as well as bottom lighting from beneath the tray, allowing optimal pictures to be captured. The tube lighting is used to capture the texture photos, and the bottom lighting is used to capture the angularity/form photos on a black-and-white scale. The system has the ability to move horizontally in both the x- and y-directions so that the preset coordinates on the aggregate tray can be captured by

the microscopic camera. These preset points are marked and, as seen in Figure 4.3, are the locations where aggregate particles are placed prior to testing.

For texture photos, the camera also transcends in the z-direction above each preset point until optimal focus is acquired on each aggregate surface. The system is computer automated and controlled by LabView^{TM} (version 6.1) and IMAQ Vision (version 2.5) software for motion control of the equipment and image acquisition, respectively (Al-Rousan, 2004). The imaging system can scan an aggregate sample and send the results to the computer for analysis in a matter of minutes.

The aggregate tray moves horizontally in the y-direction along the tracks, allowing transition between the rows of aggregate. The microscopic camera moves in the horizontal x-direction, allowing the camera to alternate between the columns of aggregate. As previously stated, the ability of AIMS to capture texture measurements of the aggregate relies on the camera transcending in the vertical z-direction. This vertical movement is automated to capture optimal focus of the aggregate particle surfaces. The measurements that AIMS can perform for coarse and fine aggregates are shown in Table 4.1.

Table 4.1. AIMS Measurement Capabilities for Fine and Coarse Aggregates

Fine Aggregates	**Coarse Aggregates**
Gradient Angularity	Gradient Angularity
Radius Angularity	Radius Angularity
Form 2d	Form 2d
	Form 3d
	Texture

The form of particles is measured by AIMS using two methods: form index (2d) and sphericity (3d). Masad et al. (2001) proposed the following form index to quantify the aggregate measurement of form using two dimensions of each particle:

$$\text{Form Index} = \sum_{\theta=0}^{\theta=360-\Delta\theta} \frac{\left|R_{\theta+\Delta\theta} - R_{\theta}\right|}{R_{\theta}} \tag{3}$$

where the R_θ variable denotes the radius of the particle being measured at an angle of θ. The incremental change in the particles radius is expressed by $\Delta\theta$.

The second technique AIMS uses to measure form is known as sphericity (Krumbein, 1941). This measurement is used to quantify the form measurement of particles using all three dimensions of an aggregate particle. The sphericity measurement is denoted by the following equation:

$$\text{Sphericity} = \sqrt[3]{\frac{d_s * d_i}{d_l^2}} \tag{4}$$

where d_s is the short dimension of the particle, d_i is the intermediate dimension, and d_l is the long dimension.

AIMS also uses two methods to measure the angularity of aggregate particles. The first method used is referred to as radius angularity. This method of characterizing angularity was developed by Masad et al. (2001). This technique measures the difference between a particle's radius and that of an equivalent ellipse in the same direction. This angularity index can be described by Equation 5:

$$\text{Angularity Index} = \sum_{\theta=0}^{\theta=360-\Delta\theta} \frac{\left|R_{P\theta} - R_{EE\theta}\right|}{R_{EE\theta}} \tag{5}$$

where $R_{P\theta}$ denotes the radius of the particle at an angle of θ and $R_{EE\theta}$ denotes the radius of an equivalent ellipse at the same angle θ (Masad et al., 2001).

AIMS also measures the angularity of aggregate particles using a gradient method. This method characterizes particles based on comparing the curvature of aggregate particles to that of a round particle. Particles that contain sharp edges rapidly change in curvature, which deviates largely from that of a round particle, which has a smooth change in curvature. Angularity is measured using a gradient angle labeled as θ and a magnitude of difference between the aggregate particle and round particle labeled as $\Delta\theta$. The angularity value is taken to be the sum of all the boundary points around the edge of the particle, which is denoted as the gradient index (GI) (Chandan et al., 2004), and can be described by the following equation:

$$GI = \sum_{i=1}^{N-3} \left| \theta_i - \theta_{i+3} \right| \tag{6}$$

where N denotes the total number of boundary points at the edge of the particle and i denotes the i^{th} point on the edge of the particle. Figure 4.4 illustrates the difference in gradient vectors between round and angular objects.

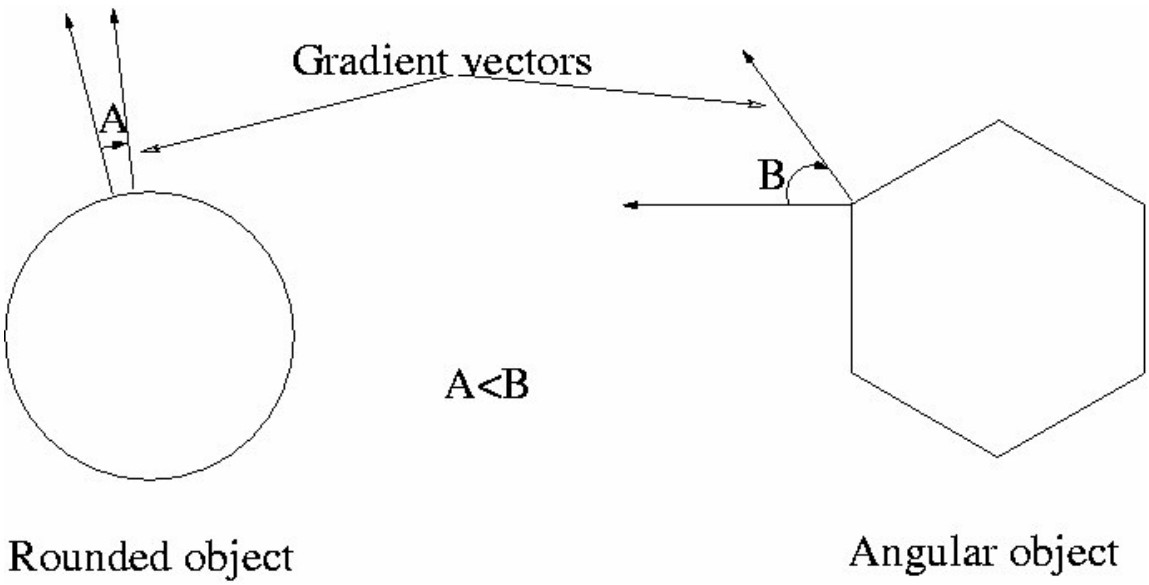

Fig. 4.4. Illustration of the difference in gradient vectors between particles (Chandan et al., 2004)

The texture property of aggregate particles is measured by AIMS using wavelet analysis. This analysis incorporates the use of frequency functions to measure the fine and coarse variations in texture. Two functions are used to denote these variations: short high-frequency waves and long low-frequency waves. Three coefficients denote the directional texture information. The first is labeled HH, which denotes high-frequency content in the diagonal direction. Coefficient LH denotes high-frequency content in the vertical direction, and coefficient HL stands for high frequency content in the horizontal direction. Texture index is denoted by the following equation:

$$Texture\ Index_n = \frac{1}{3N}\sum_{i=1}^{3}\sum_{j=1}^{N}\left(D_{i,j}(x,y)\right)^2 \quad (7)$$

This equation requires a double summation, as two variables change. The first variable is *i,* which denotes the three detailed images of texture (HH, LH, and HL). The second variable is *j*, which is the wavelet coefficient index. *N* denotes the level of decomposition (Masad, 2004). This wavelet analysis measurement of texture has been discussed in thorough detail by Mallat (1989), Fletcher et al. (2002), Chandan et al. (2004), and Al-Rousan (2004).

AIMS uses an analysis program that classifies and categorizes the aggregate property measurements. The AIMS computer software performs data analysis and presentation. AIMS records two primary types of aggregate property measurements: the percentage of particles in each classification group and the average shape properties of each sample. These results are recorded and automatically exported into Microsoft Excel files when the software analysis is performed.

PRESENTATION OF RESULTS BASED ON PERCENTAGE OF PARTICLES

One of the two types of measurements that AIMS produces is the percentage of particles in the classification groups. These classification groups, listed in Table 4.2 and shown in Figure 4.5, were developed by Al-Rousan (2004) based on statistical analysis of the variations of shape characteristics among many different aggregate sources.

The AIMS software plots each particle scanned as a single data point and then calculates the percentages of particles that fall within the classification groups. These values are known as the percentage of particles in the classification groups and are used,

as discussed in the following chapter, to correlate HMA performance to aggregate properties.

Table 4.2. Percentage of Particle Clusters Used by AIMS to Associate Similar Particles

Form 3d	**Form 2d**	**Radius Angularity (CRA, FRA)**	**Gradient Angularity (CGA, FGA)**	**Texture**
% Flat Elongated	% Circular Particles	% Rounded Particles	% Rounded Particles	% Polished Particles
% Low Sphericity	% Semicircular Particles	% Subrounded Particles	% Subrounded Particles	% Smooth Particles
% Medium Sphericity	% Semielongated Particles	% Subangular Particles	% Subangular Particles	% Low Rough Particles
% High Sphericity	% Elongated Particles	% Angular Particles	% Angular Particles	% Med. Rough Particles
CRA: Coarse Radius Angularity FRA: Fine Radius Angularity CGA: Coarse Gradient Angularity FGA: Fine Gradient Angularity				% High Rough Particles

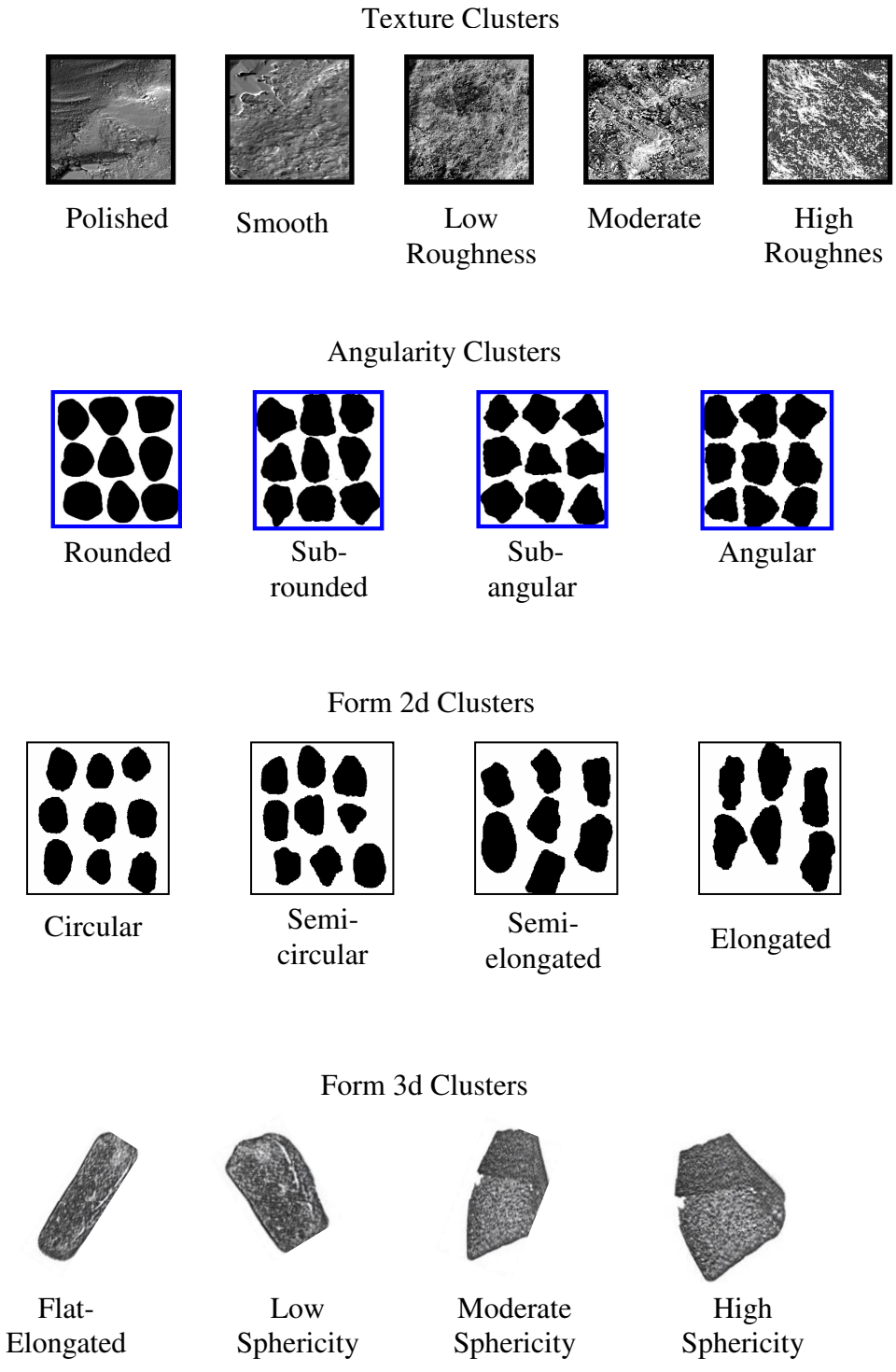

Fig. 4.5. Cluster classification charts for different aggregate properties

PRESENTATION OF RESULTS BASED ON AVERAGE SHAPE PROPERTIES

The AIMS software records the mean, standard deviation, and percentage of particles data for each aggregate particle tested. The mean value is the average value based on the number of particles tested. For coarse samples, 56 particles are always tested. For fine samples, an average of 300-400 particles are examined. The average values are also included in the analysis of the relationship of HMA performance to aggregate properties.

PRESENTATION OF RESULTS BASED ON BLEND SHAPE PROPERTIES

The weighted average of shape properties is calculated for an aggregate blend. The weights are assigned based on the surface area of each aggregate fraction for the purpose of calculating the texture and angularity properties. The surface area is estimated based on the weight of aggregate in each size fraction and by assuming particles to have a cubical shape with each dimension equal to the average size of the sieves bracketing the size fraction. The surface area is used as the weighing factor based on the assumption that smaller particles have greater surface area, and consequently, contribute more area to develop friction within the aggregate matrix. The blend form properties are calculated as a weighted average with respect to the aggregate mass in each size fraction.

CHAPTER V

STATISTICAL ANALYSIS OF THE RELATIONSHIP BETWEEN HMA PERFORMANCE, HMA VOLUMETRIC, AND AGGREGATE PROPERTIES

INTRODUCTION

The statistical analysis was performed using SPSS® release 11.5.1 software (SPSS inc., Chicago, IL). This analysis program was used to find correlations between aggregate shape and volumetric properties and HMA performance parameters. These correlations were determined separately for each of the projects discussed in Chapter III.

The statistical analysis for each project was divided into two parts. In the first part, correlations were determined among the performance parameters and the shape properties in terms of the percentages of particles in each classification group and the average properties. The second part included correlations among the performance parameters and the blend shape properties. The blend shape properties are used to calculate the angularity and texture of an aggregate blend proportion based on the surface areas of the aggregate size fractions and to calculate the form parameters of an aggregate blend based on the weights of the aggregate fractions. This chapter discuses the methods used in determining the regression correlations, the bias present in the analysis, and the SPSS® results for this research.

METHODS USED IN DETERMINING REGRESSION CORRELATIONS

SPSS® performs many statistical analysis functions. In this research, the program was used to find linear regression correlations between HMA performance parameters and volumetric and aggregate shape properties. The performance parameters were dependent variables (y-values), and the HMA volumetric and aggregate shape properties were independent variables (x-values). The x-parameters that best formed a linear regression line with respect to each performance parameter y-value were determined using SPSS®. Figure 5.1 shows the SPSS® interface used in the model construction process. The performance parameter being examined is entered in the dependent box, and all of the volumetric and aggregate shape property variables are entered in the independent box. Once the linear regression method is chosen, SPSS® analyzes the data.

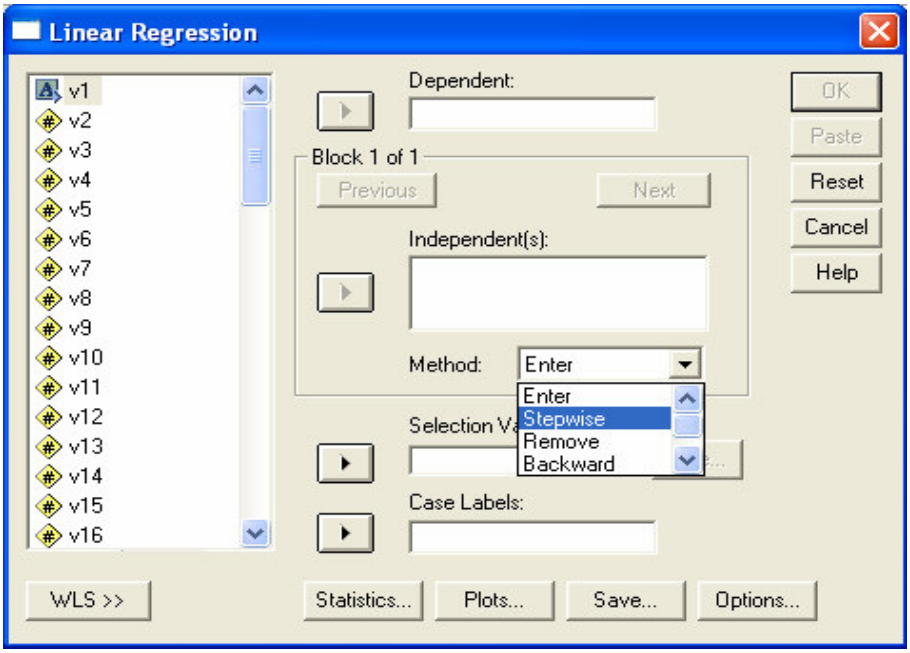

Fig. 5.1. SPSS® linear regression interface screen

There are multiple methods for determining which variables best fit the prediction model. The four types of methods that SPSS® can use, shown in Figure 5.1, are: enter, stepwise, remove, and backward. Stepwise regression was used in this research to create prediction models. This method, in a step-by-step manner, determines which volumetric and aggregate properties best predict the performance parameters by inserting and removing predictor variables in an iterative manner (Montgomery and Runger, 2003).

SPSS® uses what is known as the p-value approach to select which individual predictor variables best fit the model. In the stepwise regression method, SPSS® enters predictor variables if their individual p-value is less than the preset significance level of the test. This preset significance level is chosen by the operator and was set to a value of 0.05 in this research. The prediction variable with the lowest p-value serves as the initial prediction model. In the second step the remaining variable with the lowest p-value is added to the prediction model. Predictors added into the model may change the p-values of predictors already included in the model. This is due to factors such as collinearity in the data. Consequently, SPSS® recalculates the p-values of each predictor already included in the model every time a new predictor value is added. If any of the previous predictor p-values increase to a value greater than 0.10, that predictor is removed from the prediction model. The value at which variables are removed from the prediction model is nominally set at 0.10, but this value can be altered by the operator. Model construction is complete when no additional predictor variables can be added to the

model. This occurs when the p-values of all remaining predictor variables are larger than 0.05 (Montgomery and Runger, 2003).

PRESENCE OF BIAS IN THE STATISTICAL ANALYSIS

Bias is an effect that alters statistical estimates. Such bias prevents statistical estimates from representing true value (Montgomery and Runger, 2003). Bias should not be confused with systematic error, which is the difference between an estimated value and the true value (Phillips et al., 2001). Bias is not always avoidable and can result from all of the following: nonrandom or variant sampling, measurement and equipment problems, recording errors, approximations used in making inferences, incorrect model assumptions or model choice, and dependence between observations. Data used in this research contained properties of mixes selected randomly to represent a wide range of mixes used in the field. Therefore, the lack of statistical design in the experiments contributed to the introduction of statistical bias in this research. For example, VMA is known to be an important factor in influencing HMA mix performance. However, as will be shown in the following chapter, VMA was rarely included in the statistical correlations. This is attributed to the fact that the mixes studied did not contain a wide range of VMA measurements. As a result, the statistical analysis found few correlations between VMA values and performance measurements. Proper experimental design would have introduced mixes with significant differences in VMA values as well as other volumetric properties.

The bias present in this research can be simplified into two types: additive bias and multiplicative bias. These two types of bias differ in the manner in which they accumulate. Figure 5.2 illustrates additive bias on a plot of predicted versus measured performance measurements. The dotted line in Figure 5.2 is a 45° reference line on which the data would fall in an unbiased condition. The data are best fitted with a trend line, which is shown above the reference 45° line. The equation and R^2 fit of the trend line are also shown in Figure 5.2. The trend line in this illustration appears to be at an offset from the 45° line. The slope of the trend line is approximately 1 (0.9127), which is equivalent to the slope of the 45° line. However, the y-intercept of the trend line (0.9682) is significantly different than the y-intercept of the reference line which is at 0. This y-intercept offset is a result of additive bias. The bias in this illustration is added to each experimental point, resulting in all of the points being offset by a certain amount.

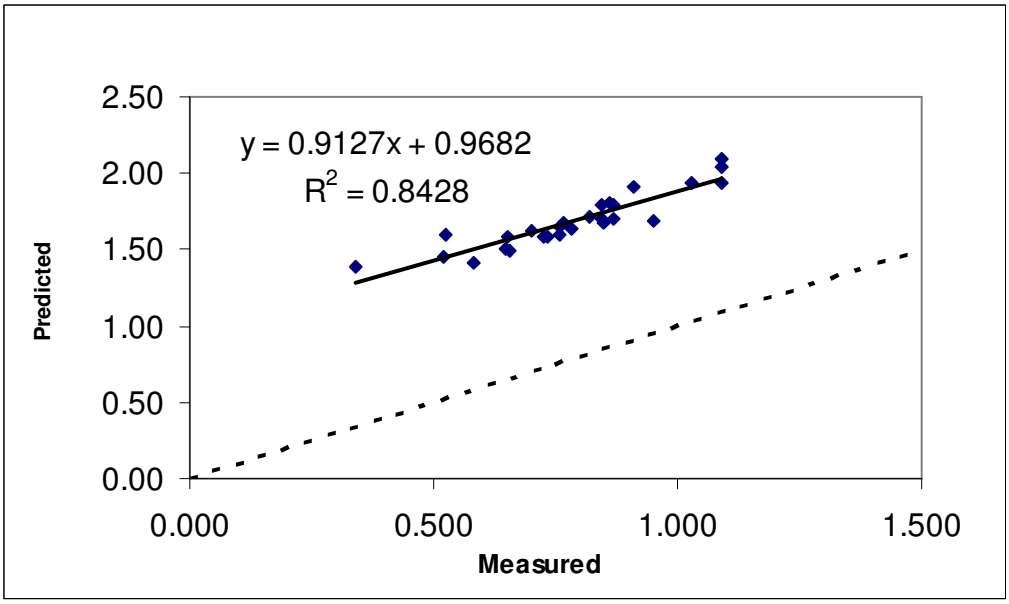

Fig. 5.2. Illustration of additive bias resulting with a Y-intercept offset

The second type of bias seen in some of the SPSS® results is multiplicative bias. This type of bias results in more bias at larger measurement values. Such bias can be seen in Figure 5.3.

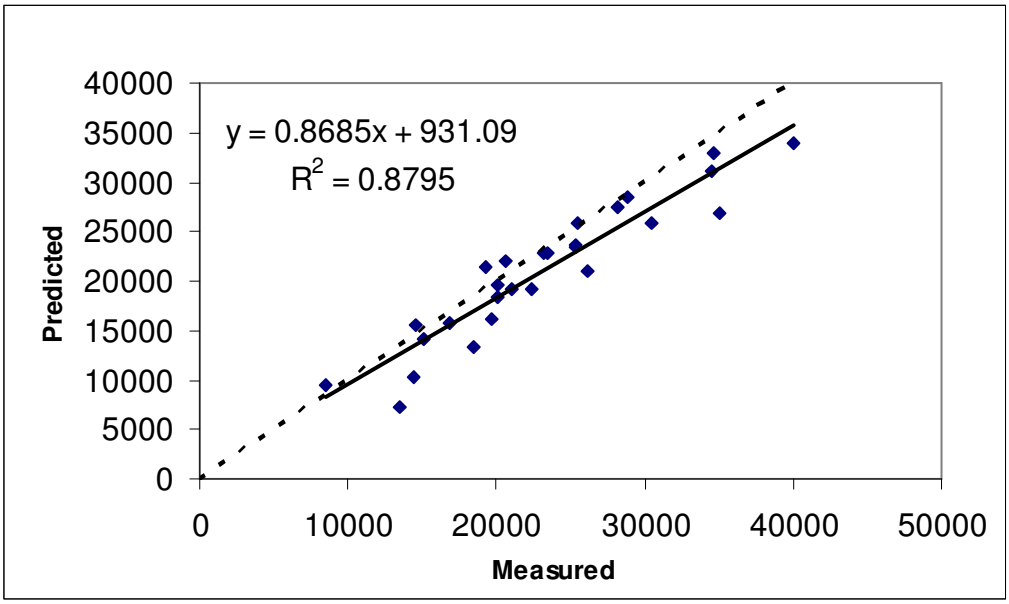

Fig. 5.3. Illustration of multiplicative bias resulting with a slope offset

As seen in Figure 5.3, the trend line deviates more from the 45° reference line as measurement values increase. Initially, the data lie on or fairly close to the 45° reference line. However, as the measurement values increase, the data begin to deviate farther and farther from the 45° reference line. This increasing deviation is due to the slope of the trend line (0.8685). This is an example of multiplicative bias in the results. A small bias is present at the lower measurement values, while much larger bias is present at the larger measurement values.

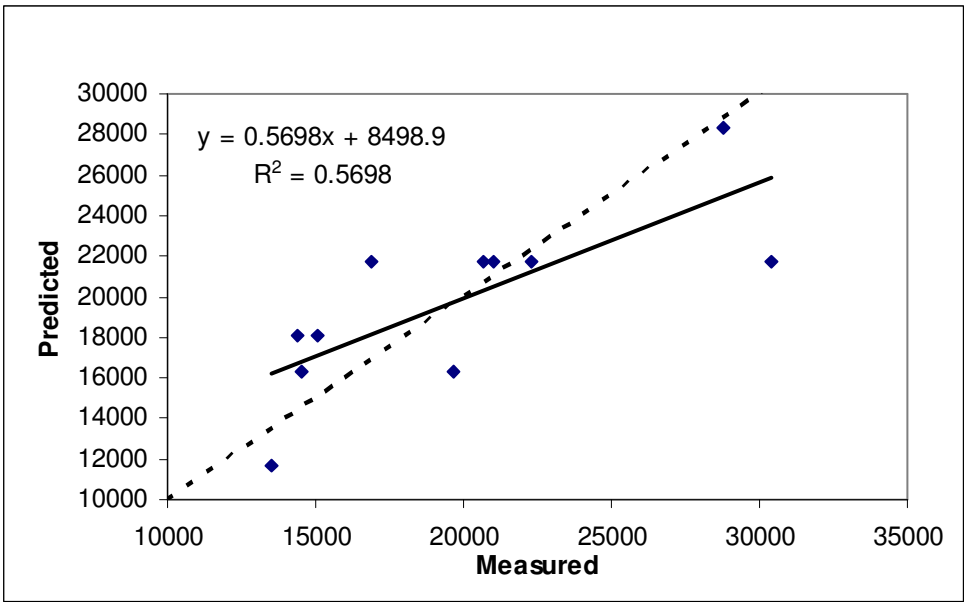

Fig. 5.4. Illustration of additive and multiplicative biases resulting with slope and Y-intercept offsets

Both types of bias can be present in some situations; such is the case in Figure 5.4. This example expresses both types of bias in the results. This is likely the result of the poor R^2 fit of the trend line. However, disregarding the poor R^2 correlation of the data, Figure 5.4 shows the presence of both multiplicative and additive biases.

AVERAGE PROPERTIES AND PERCENTAGE OF PARTICLES IN THE CLASSIFICATION GROUPS

The first part of the statistical analysis determined correlations among the performance parameters and the shape properties in terms of the percentages of particles in each classification group and the average properties. This analysis was conducted for each of the three projects examined in this research.

FHWA Mobile Laboratory Project

The FHWA mobile laboratory project was the first project examined. Table 5.1 gives the SPSS® results for the FHWA mobile laboratory project for this particular analysis. Table 5.1 lists which volumetric and aggregate properties were found to best predict each performance parameter, as well as the R^2 fit values corresponding to each initial and additional predictor variables in the stepwise regression.

The R^2 values shown in these tables are cumulative. For instance in Table 5.1, the first performance measurement, flow point, is shown with the predictor variable #22 in the initial model. This is the variable that attained the lowest p-value in the stepwise regression analysis. This single variable has an R^2 fit value of 0.567. In the second phase of the stepwise regression, SPSS® added the remaining variable with the lowest p-value to the model, variable #38. The R^2 fit value of 0.820 denotes the fit of both variables #22 and #38 to the model. Likewise, when variable #19 is added, the resulting R^2 fit value of 0.853 describes the fit of variables #22, #38, and #19 to the model.

The bottom region of Table 5.1 lists the variables that were found to correlate with each performance parameter. Variable #22, from Table 5.1, is the temperature at which the performance parameter was measured. Likewise, variables #38 and #19 represent form 2d coarse percent semicircular particles and G*, respectively. The x column lists the volumetric and aggregate property measurements that were found to best fit the performance measurements. The *B* (beta) column is the linear equation coefficients as shown in Equation 8:

$$y = \text{Constant} + B_1x_1 + B_2x_2 + \ldots + B_nx_n \quad (8)$$

The *y* value of this equation is the predicted measurement response for each performance parameter. The constant and *B* values are calculated using SPSS® and input into Equation 8. The resulting values are plotted against the measured performance parameters. These predicted versus measured performance measurements are shown in Figures A1-A30 in the Appendix. These graphs are plotted against a trend line used to calculate the R^2 fit of the data.

Figures A1-A6 present plots of measured versus predicted performance measurements for the FHWA mobile laboratory project. The R^2 fit values shown in Figures A1-A6 are the same values as those produced in the SPSS® output shown in Table 5.1. The remaining tables in the Appendix are for the other projects, which will be discussed later in this chapter.

It is evident from Table 5.1 that volumetric properties are very important in predicting performance parameters. The performance results for the FHWA mobile laboratory project were also highly dependent on the PPMT prediction variable. However, discussion will focus on the influence of aggregate shape properties.

Table 5.1. SPSS® Results for the FHWA Mobile Laboratory Projects Using Average Properties and Percentage of Aggregates in the Classification Groups

Performance Parameter	Flow Point			Strain @ Flow			Total Accumulated Strain		
Value	**x**	***B***	**R^2**	**X**	***B***	**R^2**	**x**	***B***	**R^2**
Regression Order	22	-290	0.567	22	1,199	0.524	22	1,302	0.491
	38	141	0.820	15	469	0.729	38	-882	0.752
	19	2,338	0.853	50	2,674	0.843	19	-12,599	0.799
	44	99	0.881	45	-505	0.880			
Performance Parameter	N Failure			Flow Slope (Equation 1)			Flow to Termination Slope (Equation 2)		
Value	**x**	***B***	**R^2**	**X**	***B***	**R^2**	**x**	***B***	**R^2**
Regression Order	22	-370	0.619	22	0.05	0.621	22	-0.02	0.525
	38	640	0.796	40	-0.06	0.828	16	0.08	0.711
	17	-1,363	0.853				50	-0.04	0.840
	28	-66	0.912				29	-0.01	0.880
	54	459	0.946						

Variable Notation	**Predictor Variables, x**
	15 VFA
	16 Design VTM
	17 VTM when Tested
	19 G*
	22 PPMT
	28 Texture % Polished Particles
	29 Texture % Smooth Particles
	38 Form 2d Coarse % Semicircular Particles
	40 Form 2d Coarse % Elongated Particles
	44 CRA % Angular Particles
	45 FGA % Rounded Particles
	50 Form 2d Fine % Semicircular Particles
	54 FRA % Subrounded Particles

Note: The *B* values correspond to the final prediction model.

Flow Point

The first predicted performance parameter shown in Table 5.1 is flow point. A positive correlation was established between the flow point performance parameter and the two aggregate shape properties: form 2d coarse percent semicircular particles and coarse radius angularity (CRA) percent angular particles. This is shown by the positive *B* values shown in Table 5.1. Flow point was previously described as the number of cycles an asphalt sample can withstand before revealing shear deformation. It is quite evident that a larger percentage of angularity in coarser aggregate particles will improve the flow point parameter. More angular particles provide a larger surface for asphalt to bind onto as well as increase mix friction to resist shear stresses.

The increase in percentage of semicircular particles was found to correspond to a decrease in percentage of circular particles, whereas there was very little correlation with the percentage of semielongated and elongated particles. Therefore, the positive correlation between flow point and the percentage of semicircular particles is an interesting result that can shed light on the suitability of laboratory tests to evaluate the influence of the percentage of flat particles. In this test, the performance was quantified by the one-dimensional behavior of the mix without considering deformation in the radial direction. Flat particles tend to orient such that their longest axes are in the horizontal direction, as shown in Figure 5.5. This alignment increases contact among particles perpendicular to the applied vertical load. This anisotropic behavior of the mix translates to higher stiffness in the vertical direction when compared to the horizontal direction. Hence, using a performance parameter based on the mix response in the

vertical direction might not reflect the actual behavior of the mix under the boundary conditions that exist in the field.

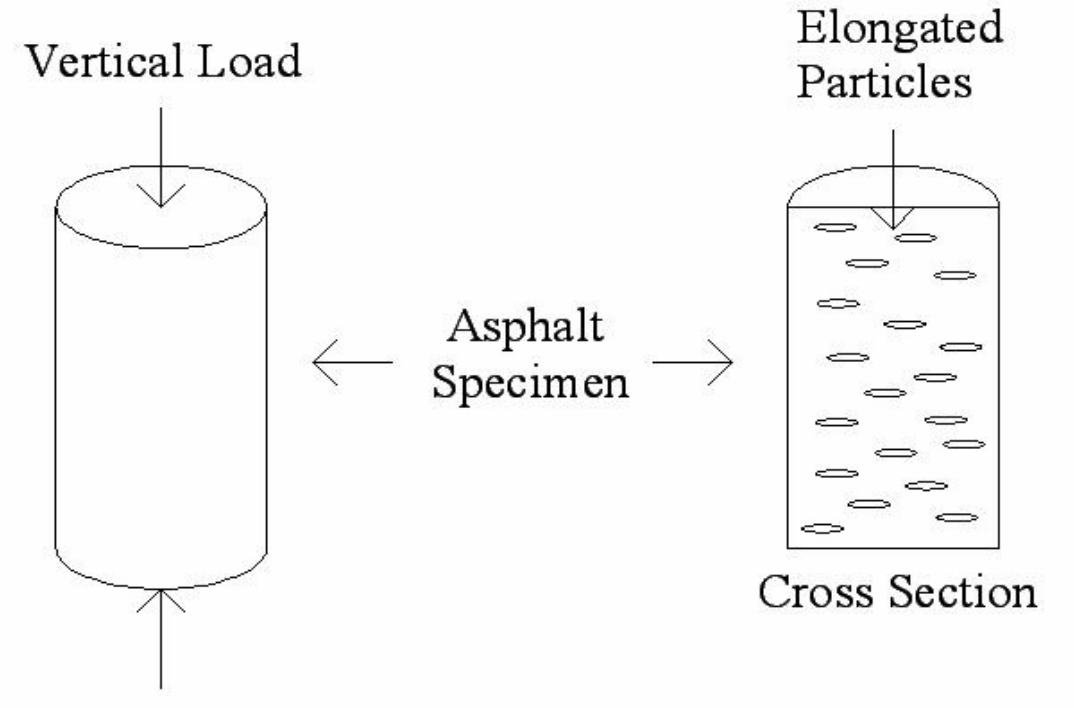

Fig. 5.5. Illustration of elongated particle orientation in laboratory specimen testing leading to anisotropic behavior in the mix

Strain @ Flow

The second performance parameter examined in the FHWA mobile laboratory project is strain @ flow. SPSS® identified a positive correlation between the strain @ flow performance parameter and the form 2d fine percent semicircular particles aggregate shape property. A negative correlation existed with the fine gradient angularity (FGA) percent rounded particles aggregate shape property. The strain @ flow value is the strain an asphalt mix attains at the flow point. Therefore, it is the strain in an

asphalt specimen when the sample begins to exhibit an increase in the rate of shear deformation. The first aggregate shape property listed in Table 5.1 is form 2d fine percent semicircular particles.

The significance of the influence of shape characteristics on strain @ flow cannot be substantiated without evaluating their effect on flow point. An increase in strain with a decrease in flow point value indicates that the mix is becoming less resistant to deformation, whereas a high strain value at a high flow point value may indicate that the mix can sustain high deformation before it becomes unstable due to applied loads. Increasing the form 2d fine percent semicircular particles was found to increase the flow point value; therefore, it is not strange for this aggregate property to improve strain @ flow. The elongation of fine particles is expected to have very little influence on the anisotropic behavior of the mix. Therefore, the discussion of the influence of coarse aggregate form might not be applicable to the fine aggregate form.

The second aggregate property listed is FGA percent rounded particles. A negative correlation was found between rounded particles and strain @ flow. An increase in round fine aggregate particles resulted in a decrease in strain the asphalt sample could withstand. Further investigation of this relationship revealed that this fine aggregate property lowered the flow point of the sample, and in so doing, decreased strain @ flow as well. Thus, it seems reasonable that the FGA percent rounded particles property had a negative correlation with the strain @ flow performance measurement.

Total Accumulated Strain

Only one aggregate property affected the prediction of total accumulated strain. A negative correlation existed between the predicted total accumulated strain and the form 2d coarse percent semicircular particles aggregate property. As the percentage of semicircular particles increased, the number of cycles to failure increased, as shown in the next section, and the total accumulated strain decreased. This finding emphasizes the correlation between aggregate form and permanent deformation.

N Failure

Three aggregate properties correlated with the number of cycles at failure. The first is form 2d coarse percent semicircular particles. This aggregate property exhibits a positive correlation with the N failure performance measurement. An increase in semicircular particles resulted with an increase in the number of cycles to failure.

The second aggregate property that correlated with this performance parameter was percent polished particles. This aggregate property exhibits a negative correlation with the N failure performance measurement, which seems quite reasonable. Polished particles have far less internal friction when compared to rougher particles. Consequently, a larger percentage of polished particles decreases the total number of cycles to failure.

The third aggregate property listed is fine radius angularity (FRA) percent subrounded particles. This aggregate property expressed a positive correlation with the N failure performance measurement. Initially, this seems to be counterintuitive.

However, upon careful examination of the data, it was found that the aggregates used in this project had comparable percentages of subangular and angular particles. The primary difference between the aggregates used in this project was in the percentages of rounded and subrounded particles. In other words, an increase in subrounded particles was a favorable property for this project.

TTI Project 9-558

The SPSS® results for this project can be seen in Table 5.2. This table lists the volumetric and shape property variables that were found to best predict each performance parameter. The predicted versus measured performance measurement graphs for each performance parameter in this project can be seen in Figures A13-A17 in the Appendix.

Compliance

The first performance parameter examined was the compliance. The results for this performance parameter, as well as the others in this project, are shown in Table 5.2. One aggregate property, form 2d coarse percent semicircular particles, was found to correlate to compliance. This positive correlation shows that an increase in semicircular particles in the asphalt sample will result in an increase in the compliance measurement of that sample.

Table 5.2. SPSS® Results for Project 9-558 Using Average Properties and Percentage of Particles in the Classification Groups

Performance Parameter	Compliance			Strain @ Flow			E*/sin ϕ at 10 Hz			APA Rut Depth (in)			Flow Point		
Value	**X**	***B***	**R^2**	**x**	***B***	**R^2**	**x**	***B***	**R^2**	**x**	***B***	**R^2**	**x**	***B***	**R^2**
Regression Order	19	-0.01	0.82	18	0.07	0.74	26	-0.01	0.47	44	0.08	0.59	26	0.29	0.52
	35	0.01	0.93	15	0.06	0.90	19	0.02	0.81	15	0.11	0.79	35	-0.79	0.85
				21	0.00	0.99									
				36	0.00	1.00									

Variable Notation	**Predictor Variables, x**
	15 VMA
	18 Asphalt Content
	19 High PG Temperature
	21 % Flat-Elongated Particles
	26 Texture % Smooth Particles
	35 Form 2d Coarse % Semicircular Particles
	36 Form 2d Coarse % Semielongated Particles
	39 CRA % Subrounded Particles
	44 FGA % Subangular Particles

Note: The *B* values correspond to the final prediction model.

A plot of the elongated particles versus the semicircular and circular particles under the form 2d measurement is shown in Figure 5.6. An increase in semicircular and circular particles correlate with a decrease in elongated particles, leading to the inference that an increase in semicircular particles, or decrease in elongated particles, results in an increase in compliance. This is consistent with the findings from the FHWA mobile data that an increase in elongated particles could increase the stiffness in laboratory tests that rely on axial deformation measurements only.

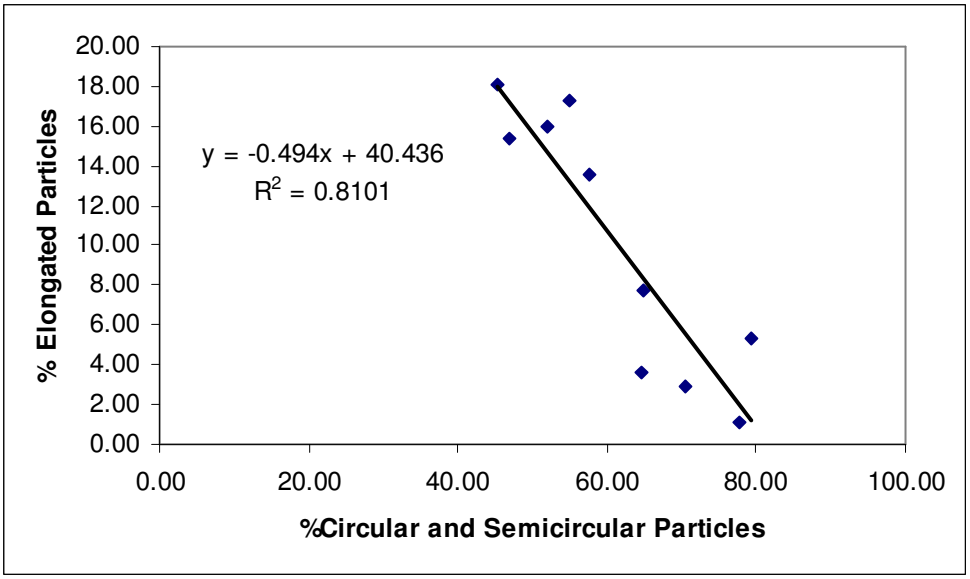

Fig. 5.6. Relationship between % elongated particles and % circular and semicircular particles

Strain @ Flow

The second performance parameter listed in Table 5.2 is strain @ flow, the total permanent strain in an asphalt sample when the sample reaches its flow point. Two aggregate properties exhibited negative correlations with this strain measurement: form

3d percent flat and elongated and form 2d coarse percent semielongated particles. These two parameters quantify the same property but in three dimensions and two dimensions, respectively. It was found that an increase in the percentage of elongated particles caused a decrease in strain @ flow, which again can be attributed to the effect of coarse aggregate form on the anisotropic behavior of the mix, which tends to increase mix resistance to deformation in the vertical direction.

E/sinϕ at 10 Hz*

The next performance parameter, E*/sinϕ at 10 Hz, had a positive correlation with the aggregate property texture percent smooth particles. This positive correlation reveals that an increase in the number of smooth particles in a mix will result in an increase in the E*/sinϕ performance measurement. This finding was quite the opposite of what would be expected. In fact, these dynamic properties are measured at very small strain that is not expected to mobilize the aggregate structure enough to correlate between aggregate shape properties and measured mechanical properties.

APA Rut Depth

The next performance parameter examined was APA rut depth. Table 5.2 shows that the FGA percent subangular particle property exhibited a positive correlation with this performance parameter. An increase in percent subangular fine aggregate particles resulted in an increase in rut depth measurement. This is contrary to the typical finding in the literature that increasing fine aggregate angularity increases rutting resistance.

Flow Point

The final performance parameter examined in this project is flow point. A positive correlation existed between this measurement and the texture percent smooth particles aggregate property. A negative correlation existed between flow point and form 2d coarse percent semicircular particles. This shows that an increase in smooth particles in an HMA mix will result in an increase in the flow point. Careful evaluation of the results showed that the aggregates in this project generally had low texture values, and an increase in smooth particles corresponded to a decrease in polished aggregates rather than a decrease in textured aggregates. According to the correlation results, a decrease in the percent semicircular particles (an increase in elongated particles) will also increase the flow point of HMA.

TTI Project 4203

TTI Project 4203 was the final project examined in this section. Three performance parameters were examined, and the SPSS® results of the performance parameters are shown in Table 5.3. The performance parameters are the average dynamic modulus (E*), the APA rut depth, and the average indirect tension (IDT) strength. Dynamic modulus was measured at three temperatures. The predicted versus measured performance measurement graphs for each performance parameter in this section can be seen in Figures A21-A25 in the Appendix.

Table 5.3. SPSS® Results for Project 4203 Using Average Properties and Percentage of Particles in the Classification Groups

Performance Parameter	Avg E* ($x10^3$ psi)									APA Rut Depth (in)			Average IDT Strength (psi)		
	5 Hz, 40˚ F			5 Hz, 70˚ F			5 Hz, 100˚ F								
Value	**x**	***B***	**R^2**	**x**	***B***	**R^2**	**x**	***B***	**R^2**	**x**	***B***	**R^2**	**x**	***B***	**R^2**
Regression Order	46	63.25	0.743	67	-52.08	0.678	43	14.98	0.777	38	0.01	0.589	67	-10.16	0.899
	39	774.92	0.954	38	-50.97	0.862	41	139.03	0.916				40	21.21	0.970

Variable Notation	**Predictor Variables, x**
	38 VFA
	39 Design VTM
	40 VTM when Tested
	41 Asphalt Content
	43 High DSR Test Temperature
	46 Form 3d % Low Sphericity
	67 FGA % Subrounded Particles

Note: The *B* values correspond to the final prediction model.

*Average E**

The first performance parameter analyzed using SPSS® was the average E* measurement at 40°F at 5Hz. A positive correlation was found between average E* at 40°F and form 3d percent low sphericity. The positive correlation is understandable in light of previous discussion on the effect of aggregate shape on anisotropy and increasing stiffness in the vertical direction.

The second performance parameter listed in Table 5.3, similar to the first, is the average E* at 70°F. A negative correlation existed between this performance measurement and FGA percent subrounded particles. A decrease in percent subrounded particles, which corresponded to an increase in subangular and angular particles, led to an increase in the E* measurement.

The third performance parameter was the average E* value measured at 100 °F. No direct correlations were established between this performance measurement and any of the aggregate properties. These discrepancies in the relationship of E* with shape properties need further investigation. They might suggest that aggregate properties do not actually affect the E* value. The E* test is conducted at a very small strain (around 100 micro strain), which is not high enough to mobilize the frictional properties of the aggregate matrix. The APA rut depth performance measurement was also analyzed; however, no correlations were found between the APA rut depth and any aggregate properties.

Average Indirect Tension Strength

A negative correlation was found between the predicted IDT strength and the aggregate property FGA percent subrounded particles. It appears that more subrounded particles will result in a decrease in the tensile strength of HMA. The relationship between percent subrounded and rounded particles and percent angular particles is shown in Figure 5.7. This relationship depicts a negative correlation between the angular and rounded particles, which is to be expected. Therefore, a decrease in rounded particles, or an increase in angular particles, resulted in an increase in the tensile strength of the HMA.

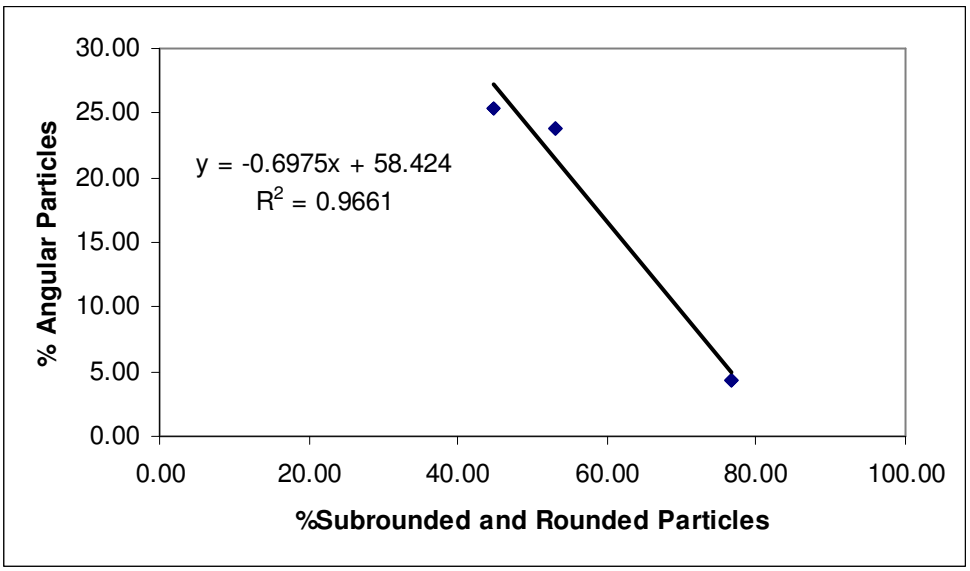

Fig. 5.7. Relationship between % angular particles and % subrounded and rounded particles

BLEND SHAPE PROPERTIES OF A MIX

The second phase of our statistical analysis incorporated the use of the blend shape properties of each mix. As mentioned above, the blend shape properties are calculated in an Excel spreadsheet and are based on the gradation of the aggregates used in each mix. The angularity and texture average values were calculated based on the percentage of the surface area of an aggregate size to the total surface area of aggregates in the blend. The surface area of each aggregate size was calculated assuming particles to be cubical in shape. The weighted averages for angularity and texture measurements were calculated based on the surface area of each size. Particles with higher surface areas have a greater influence on the blend angularity and texture. The weighted average for sphericity measurements was based on the percentage of each size by weight rather than by surface area.

One noticeable thing about the results of this analysis is that the percentage of particles in the classification groups and average property results projected a better overall fit than the blend properties results. This is due to the additional predictor variable fields in the first analysis. With fewer prediction variables in the blend properties results, there were fewer means to improve the model fitting. However, the blend properties results achieved a better fit with fewer prediction variables. The results for the flow point performance parameter from the FHWA mobile laboratory project are shown in Table 5.4.

Table 5.4. Comparison of the Flow Point Performance Parameter Results for Both Analyses

Analysis Type	**Percentage of Particles in the Classification Groups and Average Properties Results**			**Blend Shape Properties Results**		
Performance Parameter	Flow Point			Flow Point		
Value	**x**	***B***	**R^2**	**x**	***B***	**R^2**
Regression Order	22	-290	0.567	24	-254	0.597
	38	141	0.820	21	3,397	0.762
	19	2,338	0.853	14	49	0.897
	44	99	0.881			

Note: Variables are defined in Tables 5.1 and 5.5. The *B* values correspond to the final prediction model.

The percentages of particles in the classification groups and average properties results for the flow point performa7nce measurement achieved an R^2 fit of 0.853 using three predictor variables (22, 38, and 19). The blend aggregate properties results for the flow point achieved an R^2 fit of 0.897 using three predictor variables (24, 21, and 14). As mentioned, the percentage of particles in the classification groups and average properties results do in fact achieve a greater overall R^2 fit with the added prediction variable. As shown in Table 5.4, in this particular analysis the flow point performance parameter achieved an R^2 fit of 0.881 using four predictor variables (22, 38, 19, and 44).

FHWA Mobile Laboratory Project

The FHWA mobile laboratory project was examined first with respect to the blend shape properties and the results can be seen in Table 5.5. The predicted versus measured performance measurement graphs for the performance variables in this section can be seen in Figures A7-A12 in the Appendix.

Flow Point

The first performance parameter analyzed in this project was flow point. Only one aggregate property was found to have a distinct correlation with this performance measurement. This property, percent of particles with L/S >3, exhibited a positive correlation with the flow point. This is again confirming the influence of aggregate form on the anisotropic behavior of the mix; it shows that more elongation can cause higher resistance to deformation in the vertical direction in laboratory performance tests.

Table 5.5. SPSS® Results for the FHWA Mobile Laboratory Projects Using Blend Shape Properties

Performance Parameter	Flow Point			Strain @ Flow			Total Accumulated Strain		
Value	**x**	***B***	**R^2**	**X**	***B***	**R^2**	**x**	***B***	**R^2**
Regression Order	24	-255	0.597	24	729	0.570	24	1,330	0.508
	21	3,398	0.762				21	-18,604	0.709
	14	49	0.897						
Performance Parameter	N failure			Flow Slope (Equation 1)			Flow to Termination Slope (Equation 2)		
Value	**x**	***B***	**R^2**	**x**	***B***	**R^2**	**x**	***B***	**R^2**
Regression Order	24	-521	0.595	24	0.04	0.716	15	0.00	0.632
	12	-43,096	0.774	12	5.03	0.974	24	-0.01	0.807
	21	5793	0.887						

Variable Notation	**Predictor Variables, x**
	12 Sphericity
	14 % Particles w/ L/S > 3
	15 Texture
	21 G*
	24 PPMT

Note: The *B* values correspond to the final prediction model.

Strain @ Flow

The second performance parameter examined in this project was strain @ flow. No correlations existed between the strain performance parameter and the blend properties measurements. The reason for this lack of correlation is probably the result of the dominant correlation between the strain @ flow performance parameter and the volumetric predictor variable PPMT.

Total Accumulated Strain

Similar to the previous results, the total accumulated strain performance parameter also lacked correlation to any blend aggregate properties, also due to the dominant correlation between the performance parameter and the PPMT predictor variable. This performance parameter was found to be correlated to the PPMT and G* volumetric properties.

N Failure

The fourth performance parameter, N failure, was found to be negatively correlated with the aggregate property of sphericity. Sphericity is the resulting measurement of the form 3d test. The negative correlation between spherical particles and the N failure performance measurement agrees with the previous discussion about mix anisotropic behavior.

TTI Project 9-558

The SPSS® results for TTI Project 9-558 are shown in Table 5.6. These results include the performance measurements of compliance, strain @ flow, and APA rut depth. The predicted versus measured performance measurement graphs for the performance variables in this section can be seen in Figures A18-A20 in the Appendix.

Compliance

Only two of the performance parameters were found to correlate with the blend aggregate properties. The first performance parameter, compliance, was found to negatively correlate to the aggregate property measurement of radius angularity. It is reasonable that an increase in angularity would increase HMA dynamic modulus and thus decrease compliance. This is due to the gained additional bonding and friction between angular aggregates and asphalt.

Strain @ Flow

The second performance parameter shown in Table 5.6 is the strain @ flow. A negative correlation was found between this measurement and percent of particles with L/S > 3. This correlation shows that an increase in elongated particles results in a decrease in the strain in an HMA sample.

Table 5.6. SPSS® Results for Project 9-558 Using Blend Shape Properties

Performance Parameter	Compliance			Strain @ Flow			APA Rut Depth (in)		
Value	**x**	***B***	**R^2**	**x**	***B***	**R^2**	**x**	***B***	**R^2**
Regression Order	21	-0.01	0.819	20	0.08	0.739	19	9.30	0.400
	20	0.04	0.907	17	0.07	0.900			
	11	-0.04	0.969	15	-0.00	0.984			
Variable Notation	**Predictor Variables, x**								
	11	Radius Angularity							
	15	% Particles w/ L/S > 3							
	17	VMA							
	19	Design Air Voids							
	20	Asphalt Content							
	21	High PG Temperature							

Note: The *B* values correspond to the final prediction model.

APA Rut Depth

APA rut depth was found to have a positive correlation with the design air voids volumetric property. The APA rut depth did not correlate with any of the aggregate properties.

TTI Project 4203

The SPSS® results for TTI Project 4203 can be seen in Table 5.7. Similar to the previous section, the blend properties results for Project 4203 found few correlations between aggregate properties and HMA performance. Only one of the five performance parameters was found to correlate to an aggregate property. The predicted versus measured performance measurement graphs for the performance variables in this section can be seen in Figures A26-A30 in the Appendix.

The only performance parameter found to correlate to an aggregate shape property in this section is average IDT strength. The results show a negative correlation between the IDT strength and percent of particles with L/S >3. An increase in elongated particles results in a decrease in tensile strength in the HMA sample. This also results from the anisotropic behavior of the HMA mix.

Table 5.7. SPSS® Results for Project 4203 using Blend Shape Properties

Performance Parameter	Avg E* (x10^3 psi)									APA Rut Depth (in)			Average IDT Strength (psi)		
	5 Hz, 40˚ F			5 Hz, 70˚ F			5 Hz, 100˚ F								
Value	***x***	***B***	***R^2***	**x**	***B***	**R^2**	**x**	***B***	**R^2**	**x**	***B***	**R^2**	**x**	***B***	**R^2**
Regression Order	45	47.06	0.584	45	33.66	0.551	45	14.98	0.78	40	0.01	0.589	37	-1.70	0.873
				43	433.7	0.783	43	139.03	0.92						

Variable Notation	**Predictor Variables, x**
37	% Particles w/ L/S >3
40	VFA
43	Asphalt Content
45	Temperature G* was Measured

Note: The *B* values correspond to the final prediction model.

CHAPTER VI

CONCLUSIONS AND RECOMMENDATIONS

CONCLUSIONS

The analysis conducted for this thesis evaluated the influence of aggregate shape properties, among other mix properties, on a number of performance parameters measured using laboratory tests. Three databases containing results from major studies on performance evaluation of HMA mixes were included in the statistical analysis conducted for this thesis. The correlation analysis was possible with the development of AIMS, which is capable of accurately and rapidly measuring aggregate shape properties.

The analysis results indicate that aggregate shape properties play a dominant role in influencing the performance of HMA. Many of the aggregate properties were found to correlate with multiple performance parameters. The percentage of smooth particles in the texture aggregate property correlated to the performance parameters of flow point and number of cycles to failure. The form of coarse particles correlated to flow point, strain @ flow, total accumulated strain, number of cycles to failure, and compliance.

The most interesting, and probably controversial, finding is that an increase in the percentage of flat particles corresponded to an increase in resistance to permanent deformation in the vertical direction. This could be caused by the fact that elongated particles tend to orient such that the longest axes of particles are inclined toward the horizontal plane. Consequently, more contacts develop in the vertical direction. The increase in these contacts induces an anisotropic behavior of the mix, which translates to

higher stiffness in the vertical direction. This finding might suggest that axial laboratory tests might not reproduce actual field performance of aggregates with different percentages of flat and elongated particles. The reported disadvantages of using flat and elongated particles are breakage of particles and weak planes in the horizontal directions. Neither of these behaviors is captured sufficiently in axial performance tests.

The weighted average of shape properties was calculated for each aggregate blend. The weights were assigned based on the surface area of each aggregate fraction for the purpose of calculating the texture and angularity properties. The surface area was estimated based on the weight of aggregate in each size fraction and by assuming particles to have a cubical shape with each dimension equal to the average size of the sieves bracketing the size fraction. The surface area was used as the weighing factor based on the assumption that smaller particles have greater surface area, and consequently, contribute more area to develop friction within the aggregate matrix. The blend form properties were calculated as a weighted average with respect to the aggregate mass in each size fraction. The correlations with blend properties were far less pronounced than with the percentages of particles in the different classification groups.

Unfortunately, the lack of statistical design in the databases used in this research deterred the development of actual predictive equations that include aggregate shape. The excessive amount of bias in the correlations, which can be seen in Figures A1-A30 in the Appendix, prevented any predictive equations from being reformulated to include aggregate shape properties. Although this is a drawback to the extensive amount of

effort put into this research, the fact that aggregate shape properties vastly affect the performance of HMA pavements is evident. SPSS® determined that some of the aggregate shape properties were more dominant factors in predicting certain performance parameters than were the mix volumetrics. This can be seen in the SPSS® results found in Tables 5.1-5.3 and 5.5-5.7.

RECOMMENDATIONS

It is evident that aggregate shape characteristics of form, angularity, and texture influence the performance of HMA pavements. Recent studies have also shown that AIMS is capable of accurately measuring these aggregate characteristics. The inability to develop predictive equations that relate HMA performance to volumetric and aggregate properties was largely due to the original experimentation process. The development of predictive equations can only be achieved in a project designed for that purpose. Such a project must consider statistical analysis design so that all statistical assumptions are satisfied when relating aggregate shape properties and HMA performance measurements. Variations in HMA properties believed to affect performance should be included in these experiments.

The inclusion of many different types of aggregates is also needed. Larger variations between aggregate shape properties of form, angularity, and texture, in each aggregate sample would produce better results. Each aggregate would need to be examined in several different types of HMA mix designs, as well. This type of project

would require an extensive amount of time and funding, but it is the only way to properly relate aggregate shape properties to HMA performance.

REFERENCES

Al-Rousan, T. M. (2004). "Characterization of aggregate shape properties using a computer automated system." Ph. D. Dissertation, Dept. of Civil Engineering, Texas A&M University, College Station, TX.

Barrett, P. J. (1980). "The shape of rock particles, a critical review." *Sedimentology*, 27, 291-03.

Bathina M. (2005). "Quality analysis of the aggregate imaging system (AIMS) measurements." Master's Thesis, Dept. of Civil Engineering, Texas A&M University, College Station, TX.

Bhasin, A., Button, J. W., and Chowdhury, A. (2003). "Evaluation of simple performance tests on HMA mixtures from the south central USA." *TTI Report 9-558*, Texas Transportation Institute, Texas A&M University, College Station, TX.

Campen, W. H., and Smith, J. R. (1948). "A study of the role of angular aggregates in the development of stability in bituminous mixtures." *Proc. AAPT, 17*, 114-142.

Chandan, C., Sivakumar, K., Fletcher, T., and Masad, E. (2004). "Geometry analysis of aggregate particles using imaging techniques." *Journal of Computing in Civil Engineering*, ASCE, 18(1), 75-82.

Chowdhury, A., Bhasin, A., and Button, J. W. (2003). "As-built properties of test pavements on IH-20 in Atlanta District." *TTI Report 0-4203*, Texas Transportation Institute, Texas A&M University, College Station, TX.

Chowdhury, A., Button, J. W., Kohale, V., and Jahn, D. (2001). "Evaluation of Superpave fine aggregate angularity specification." *International Center for Aggregates Research ICAR Report 201-1*, Texas Transportation Institute, Texas A&M University, College Station, TX.

Field, F. (1958). "Effect of percent crushed variation in coarse aggregates of Bituminous mixes." *Proceedings, Association of Asphalt Paving Technologists,* 27, 294-322.

Fletcher, T., Chandan, C., Masad, E., and Sivakumar, K. (2002). "Measurement of aggregate texture and its influence on HMA permanent deformation." *Journal of Testing and Evaluation, American Society for Testing and Materials, ASTM*, 30(6), 524-531.

Foster, C. R. (1970). "Dominant effect of fine aggregate on strength of dense-graded asphalt mixes." *Highway Research Board Special Report 109*. Transportation Research Board, National Research Council, Washington DC, 1-3.

Gaudette, B. E., and Welke, R. A. (1977). "Investigation of crushed aggregates for bituminous mixtures." *Michigan Department of State and Highway Transportation,* Report No. TB-58, 1977.

Herrin, M., and Goetz, W. H. (1954). "Effect of aggregate shape on stability of bituminous mixes." *Proceedings, Highway Research Board, 33*, 293-306.

Huber G. A., Jones J. C., and Jackson N. M. (1998). "Contribution of fine aggregate angularity and particle shape to superpave mixture performance," *Transportation Research Record, Journal of the Transportation Research Board*, 1609, 28-5.

Ishai, I., and Gellber, H. (1982). "Effect of geometric irregularity of aggregates on the properties and behavior of asphalt concrete." *Proceedings, Association of Asphalt Paving Technologists*, 51, 494-521.

Kalcheff, I. V., and Tunnicliff, D. G. (1982). "Effect of crushed stone size and shape on properties of asphalt concrete." *Journal of Association of Asphalt Paving Technologists*, 51, 453-470.

Kaloush, K. and Witczak, M. W. (2002). "Tertiary flow characteristics of asphalt mixtures". *Journal of the Association of Asphalt Paving Technologists*, 71, 248-280.

Kandhal, P. S., and Parker, F., Jr. (1998). "Aggregate tests related to asphalt concrete performance in pavements." *National Cooperative Highway Research Program Report 405*, Transportation Research Board, National Research Council, Washington DC.

Kandhal P. S., and Wenger M. E. (1973). "Effect of crushed gravel coarse aggregate on properties of bituminous concrete." *Pennsylvania Department of Transportation. Research Report,* 70-82, Harrisburg, PA.

Kandhal, P. S., Motter, J. B., and Khatri, M. A. (1991). "Evaluation of particle shape and texture: manufactured versus natural sands." *Transportation Research Record 301*, Transportation Research Board, National Research Council, Washington, DC, 48-67.

Krumbein, W. C. (1941). "Measurement and geological significance of shape and roundness of sedimentary particles." *Journal of Sedimentary Petrology*, 11(2), 64-72.

Lefebure, J. (1957) "Recent investigations of design of asphalt paving mixtures." *Proceedings, Association of Asphalt Paving Technologists,* 26, 321-394.

Li, M. C., and Kett, I. (1967). "Influence of coarse aggregate shape on the strength of asphalt concrete mixtures." *Highway Research Record 178*, Transportation Research Board, National Research Council, Washington DC, 93-106.

Mallat, S. G. (1989). "A theory for multiresolution signal decomposition: the wavelet representation." *IEEE Transactions on Pattern Analysis and Machine Intelligence*, 11, 674-693.

Masad, E. (2003). "The development of a computer controlled image analysis system for measuring aggregate shape properties," *NCHRP-IDEA Project 77 Final Report, Transportation Research Board*, Washington DC.

Masad, E. (2004). "Aggregate imaging system (AIMS) basics and applications" *Report FHWA/TX-05/5-1707-01-1, Texas Department of Transportation and Federal Highway Administration,* Washington DC.

Masad, E., Olcott, D., White, T., and Tashman, L. (2001). "Correlation of fine aggregate imaging shape indices with asphalt mixture performance." *Transportation Research Record 1757*. Transportation Research Board, National Research Council, Washington DC, 148-156.

Masad, E., Little, D., Tashman, L., Saadeh, S., Al-Rousan, T., and Sukhwani, R. (2003). "Evaluation of aggregate characteristics affecting HMA concrete performance." *International Center for Aggregates Research ICAR Report 203-1*, Texas Transportation Institute, Texas A&M University, College Station, TX.

Maupin, G. W. (1970). "Effect of particle shape and surface texture on the fatigue behavior of asphaltic concrete." *Highway Research Record, 313*.

Monismith, C. L. (1970). "Influence of shape, size, and surface texture on the stiffness and fatigue response of asphalt mixtures." *Highway Research Board 109 Special Report,* Transportation Research Board, National Research Council, Washington DC, 4–11.

Montgomery, D. C., and Runger, G. C. (2003). "*Applied statistics and probability for engineers*," 3rd Ed., John Wiley & Sons, New York, NY.

Moore, R. B. and Welke, R. A. (1979). "Effects of fine aggregate on stability of bituminous mixes." Testing and Research Division, Testing Laboratory Section, *Michigan Department of Transportation, Research Report 78 TB-34-79F*.

Phillips, S. D., Estler, W. T., Doiron, T., Eberhardt, K. R., and Levenson, M. S. (2001). "A careful consideration of the calibration concept." *Journal of the National Institute of Standards and Technology,* 106(2), 371-379.

Rittenhouse, G. (1943). "A visual method of estimating two dimensional sphericity." *Journal of Sedimentary Petrology*, 13(2), 79-81.

Roberts, F. L., Kandhal, P. S., Brown, E. R., Lee, D., and Kennedy, T. W. (1996). "*Hot mix asphalt materials, mixture design, and construction*," 2nd Ed., NAPA Research and Education Foundation, Lanham, MD.

Sanders, C. A., and Dukatz, E. L. (1992). "Evaluation of percent fracture of hot-mix asphalt gravels in Indiana." *Effect of Aggregate and Mineral Filler on Asphalt Mixture Performance,* R. C. Meininger, Ed., American Society for Testing and Materials, STP 1147. Philadelphia, PA.

Superpave System, The (2000). Retrieved April 20, 2005, from http://www.fhwa.dot.gov/winter/roadsvr/superbro.htm

Tons, E., and Goetz, W. H. (1968). "Packing volume concepts for aggregates." *Highway Research Record 236*, Transportation Research Board, National Research Council, Washington DC, 79-96.

Wedding, P. A., and Gaynor, R. D. (1961). "The effect of using crushed gravel as the coarse and fine aggregate in dense-graded bituminous mixtures." *Proceedings, Association of Asphalt Paving Technologists*, 30, 469-492.

Winford, J. M. (1991). "Evaluation of fine aggregate particle shape and texture and its effect on permanent deformation of asphalt paving mixtures." Ph.D. Dissertation, Department of Civil Engineering, Auburn University, Auburn, AL.

Yeggoni, M., Button, J. W., and Zollinger, D. G. (1996). "Fractals of aggregates correlated with creep in asphalt concrete." *Journal of Transportation Engineering (ASCE)*, 122(1), 22-28.

APPENDIX

GRAPHS DEPICTING MEASURED VERSUS PREDICTED PERFORMANCE PARAMETERS

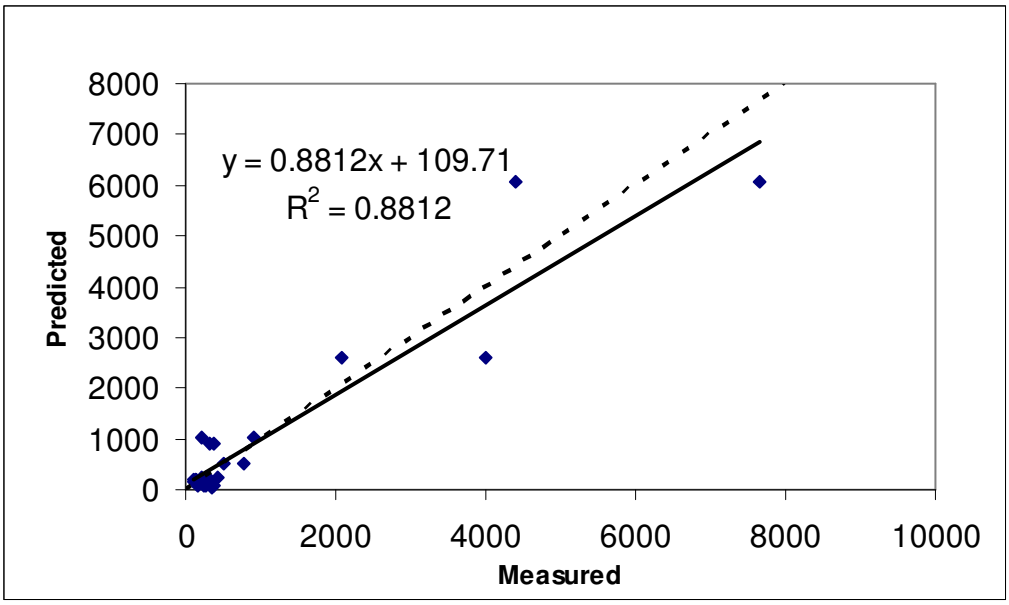

Fig. A1. FHWA mobile lab.-average properties-
flow point measured vs. predicted results

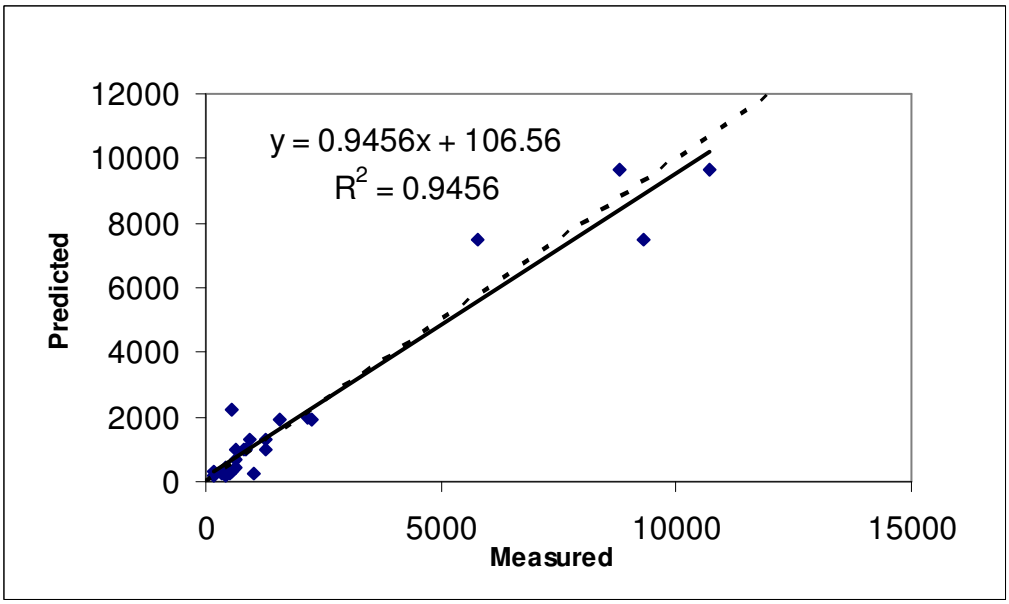

Fig. A2. FHWA mobile lab.-average properties-
N failure measured vs. predicted results

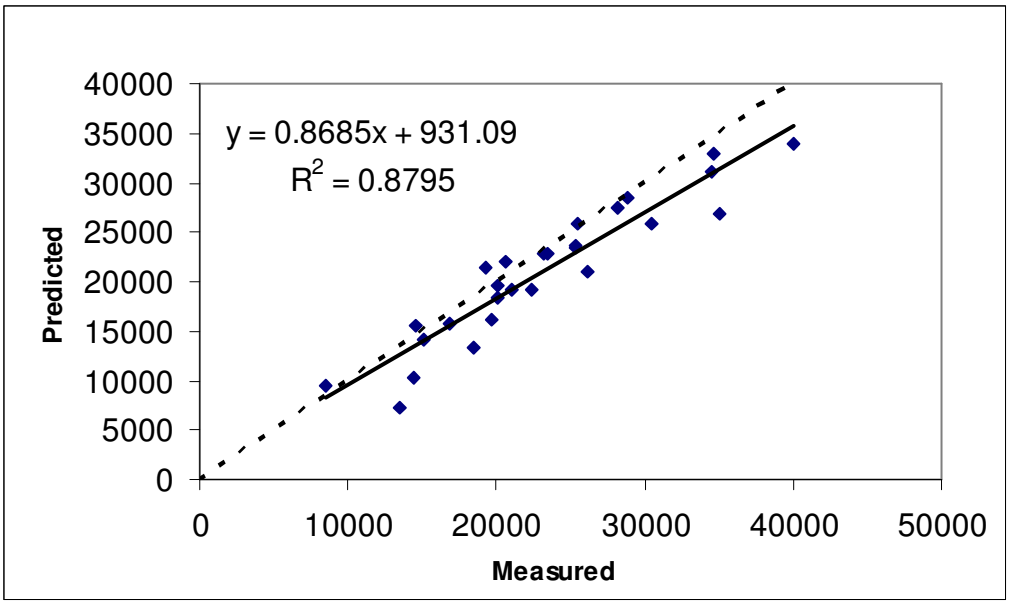

Fig. A3. FHWA mobile lab.-average properties-
strain @ flow measured vs. predicted results

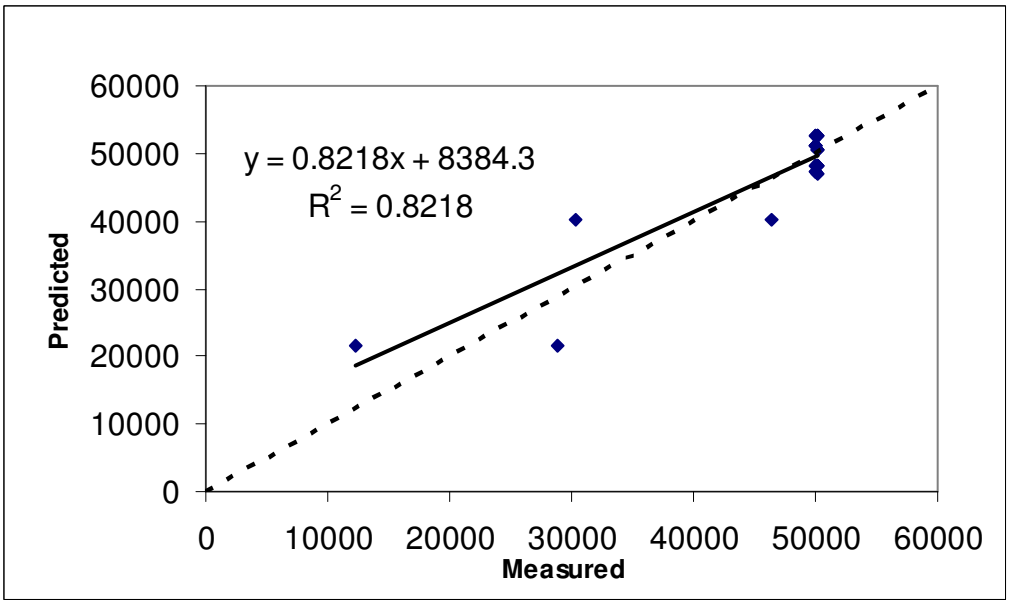

Fig. A4. FHWA mobile lab.-average properties-
total strain measured vs. predicted results

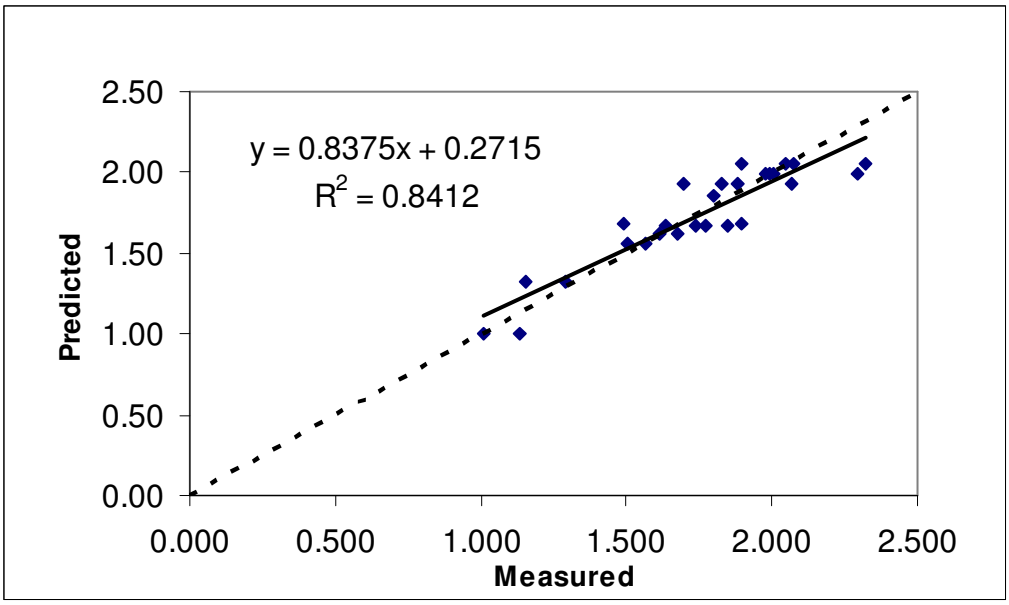

Fig. A5. FHWA mobile lab.-average properties-
flow slope measured vs. predicted results

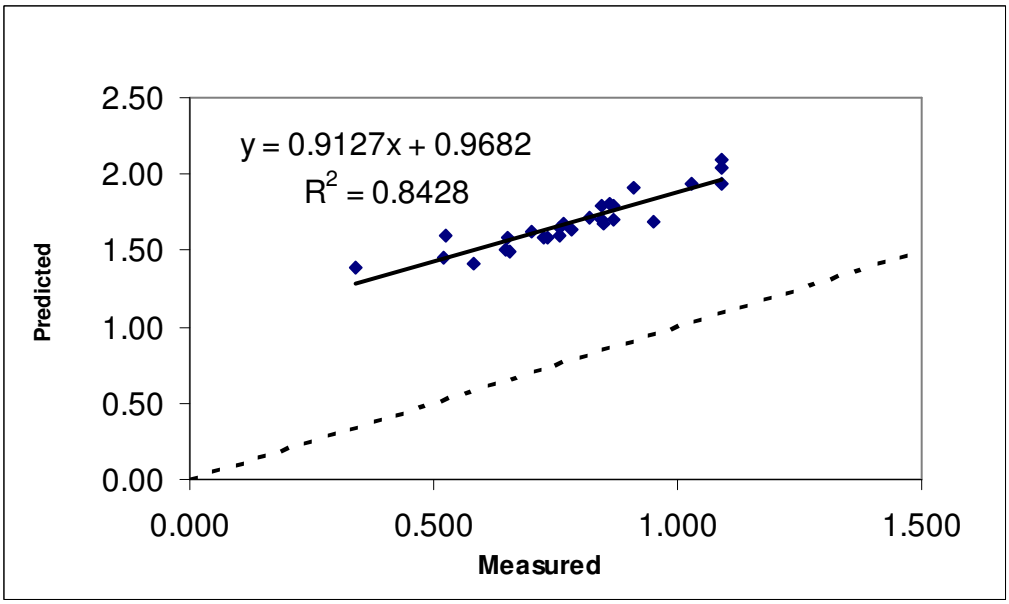

Fig. A6. FHWA mobile lab.-average properties-
flow to termination slope measured vs. predicted results

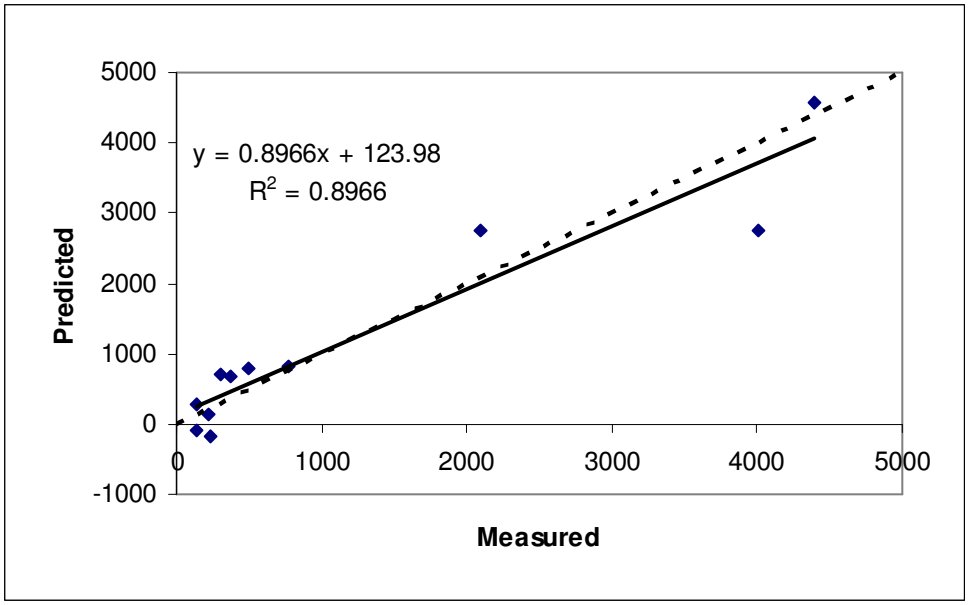

Fig. A7. FHWA mobile lab.-blend properties-
flow point measured vs. predicted results

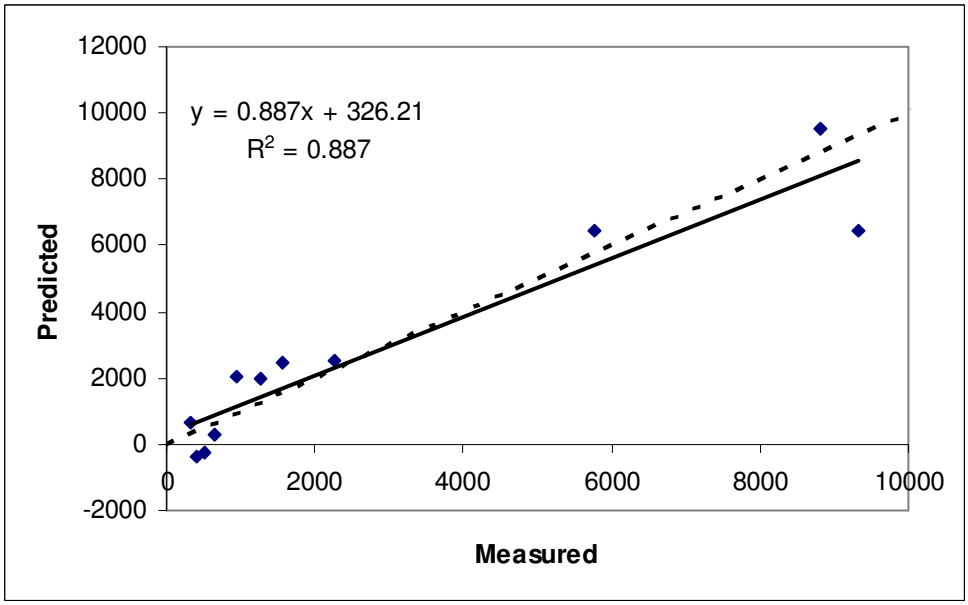

Fig. A8. FHWA mobile lab.-blend properties-
N failure measured vs. predicted results

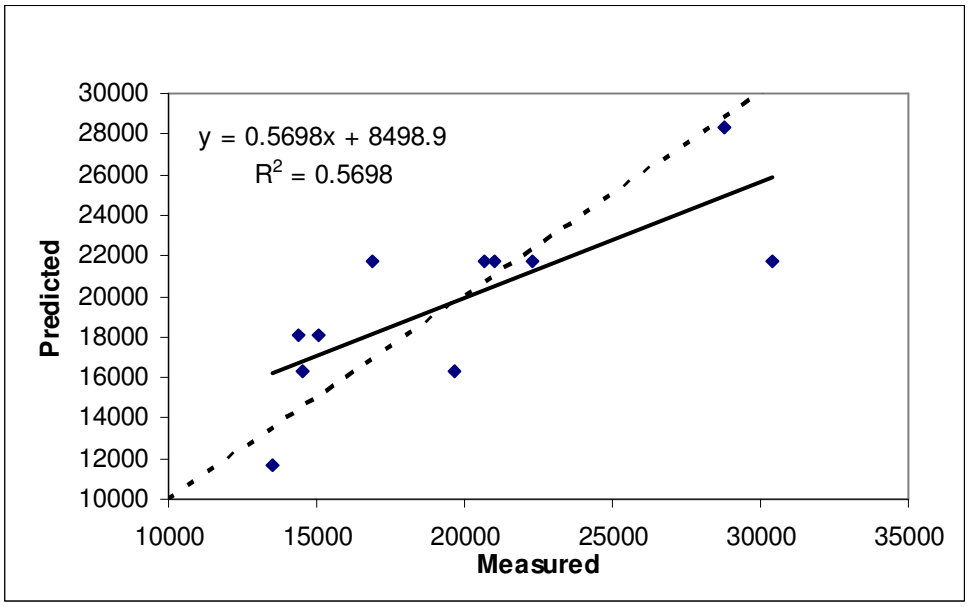

Fig. A9. FHWA mobile lab.-blend properties-
strain @ flow measured vs. predicted results

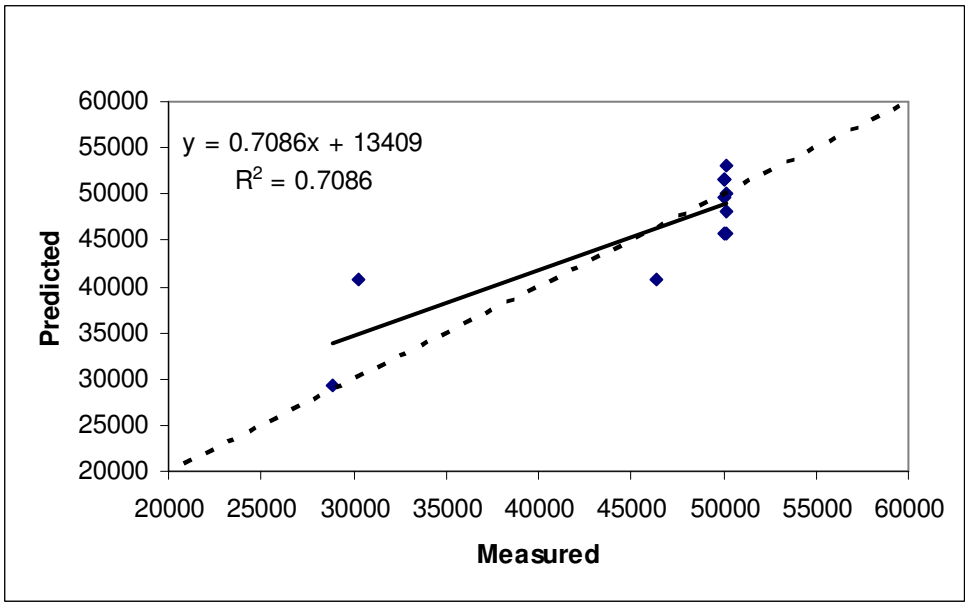

Fig. A10. FHWA mobile lab.-blend properties-
total strain measured vs. predicted results

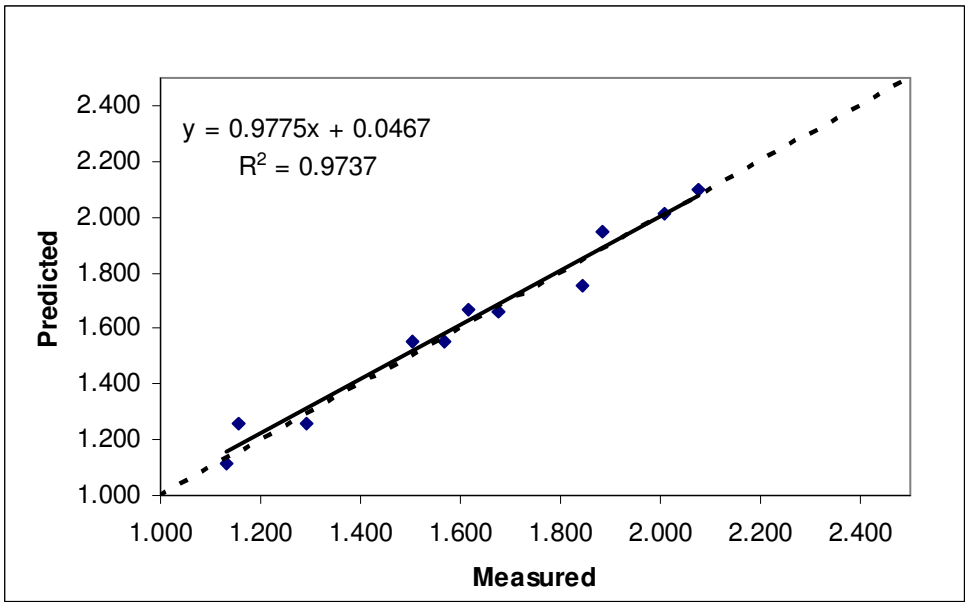

Fig. A11. FHWA mobile lab.-blend properties-
flow slope measured vs. predicted results

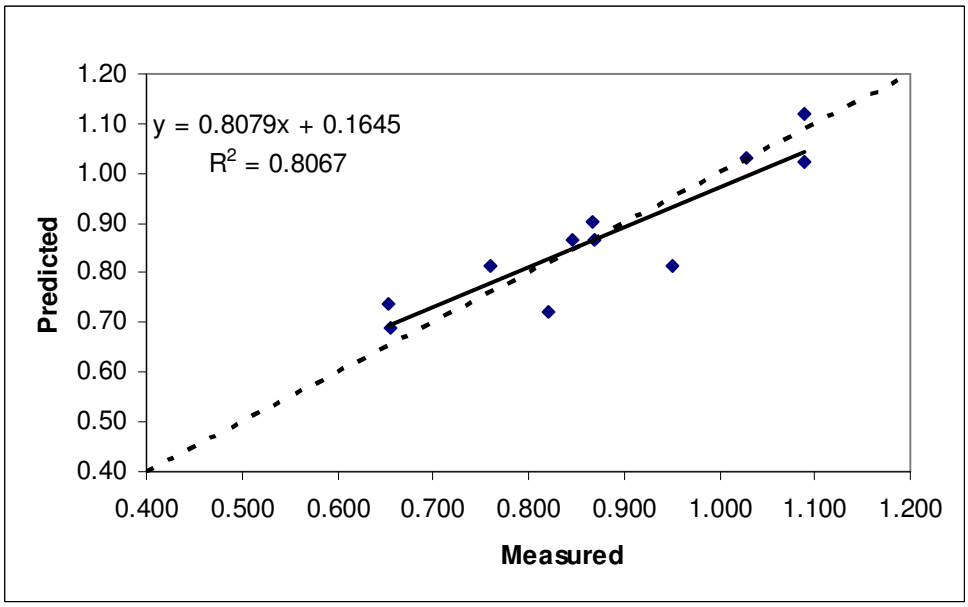

Fig. A12. FHWA mobile lab.-blend properties-
flow to termination slope measured vs. predicted results

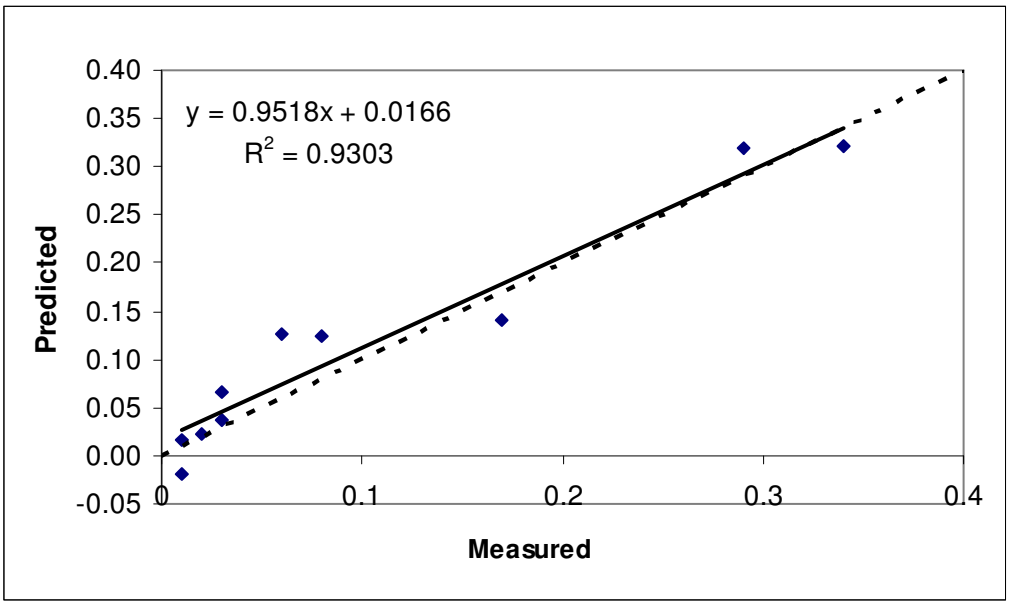

Fig. A13. Project 9-558-average properties-
compliance measured vs. predicted results

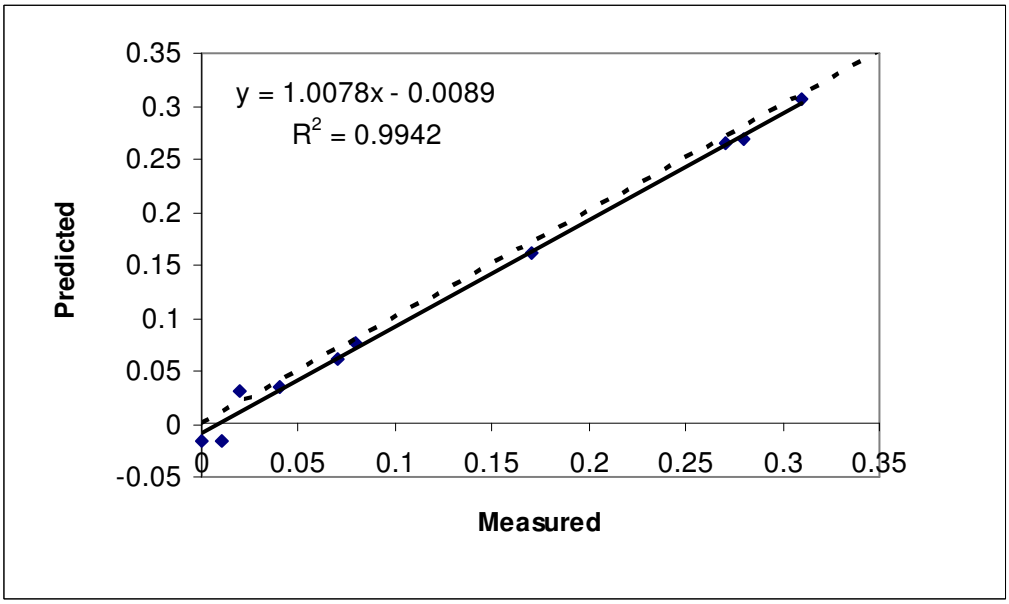

Fig. A14. Project 9-558-average properties-
strain @ flow measured vs. predicted results

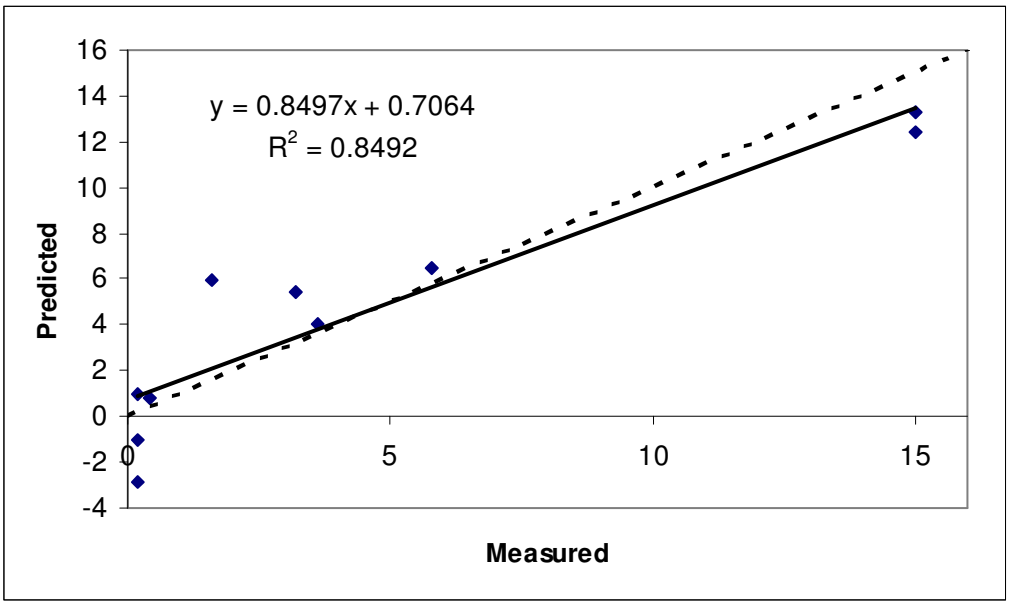

Fig. A15. Project 9-558-average properties-
flow point measured vs. predicted results

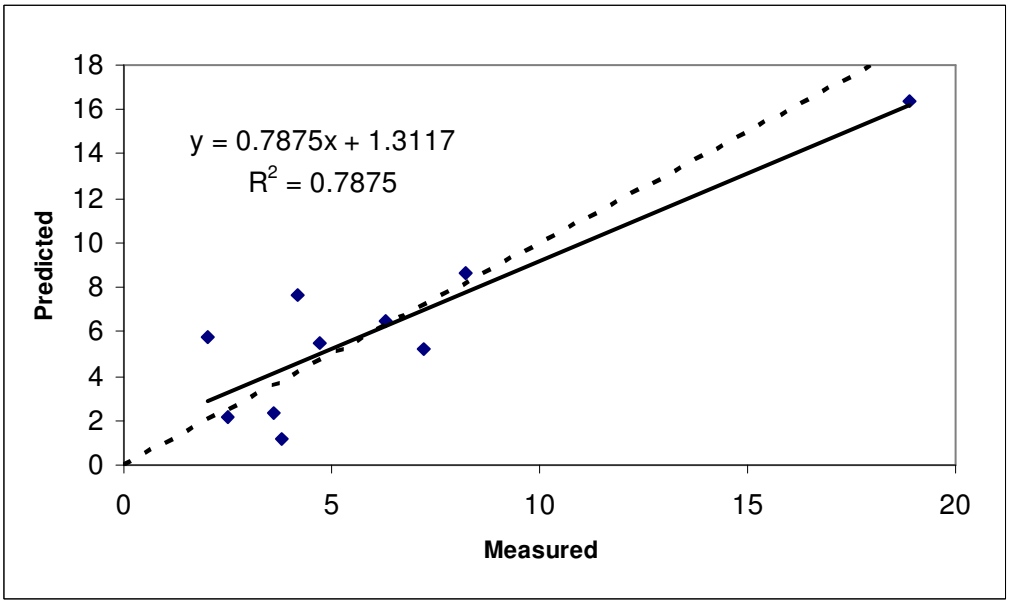

Fig. A16. Project 9-558-average properties-
APA rut depth measured vs. predicted results

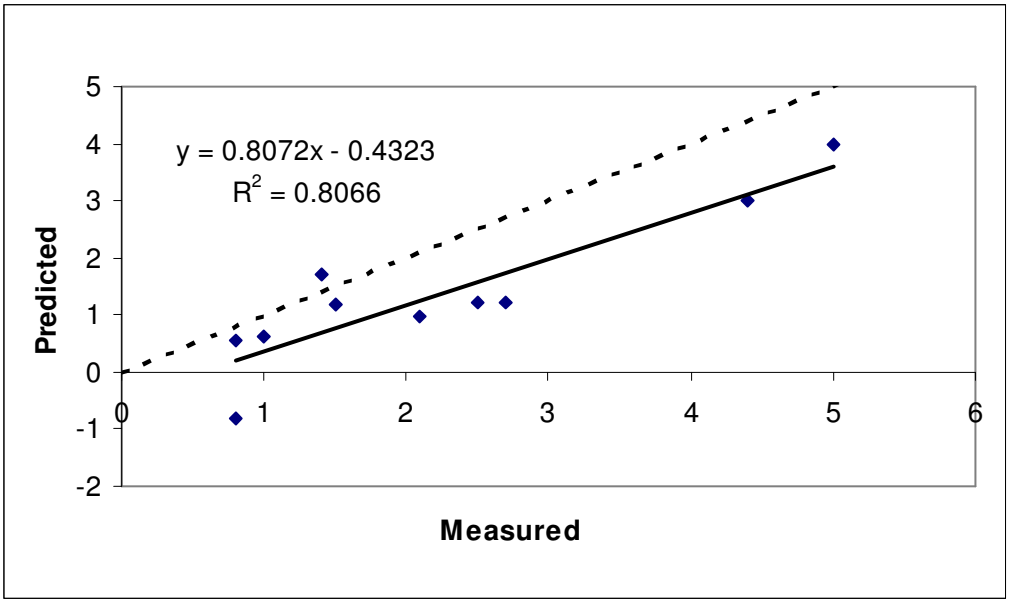

Fig. A17. Project 9-558-average properties-
E*/sin Φ measured vs. predicted results

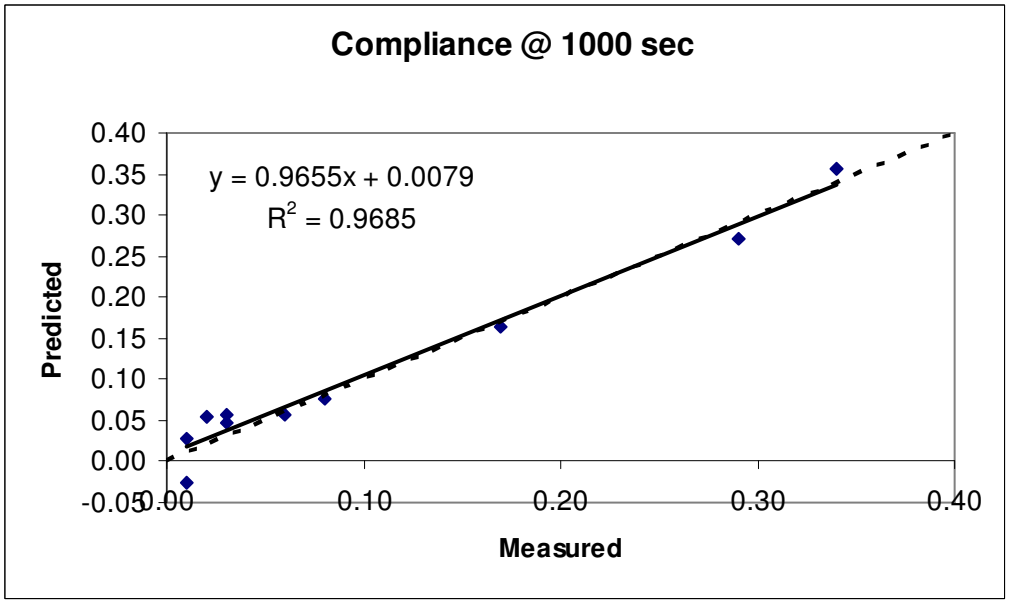

Fig. A18. Project 9-558-blend properties-
compliance measured vs. predicted results

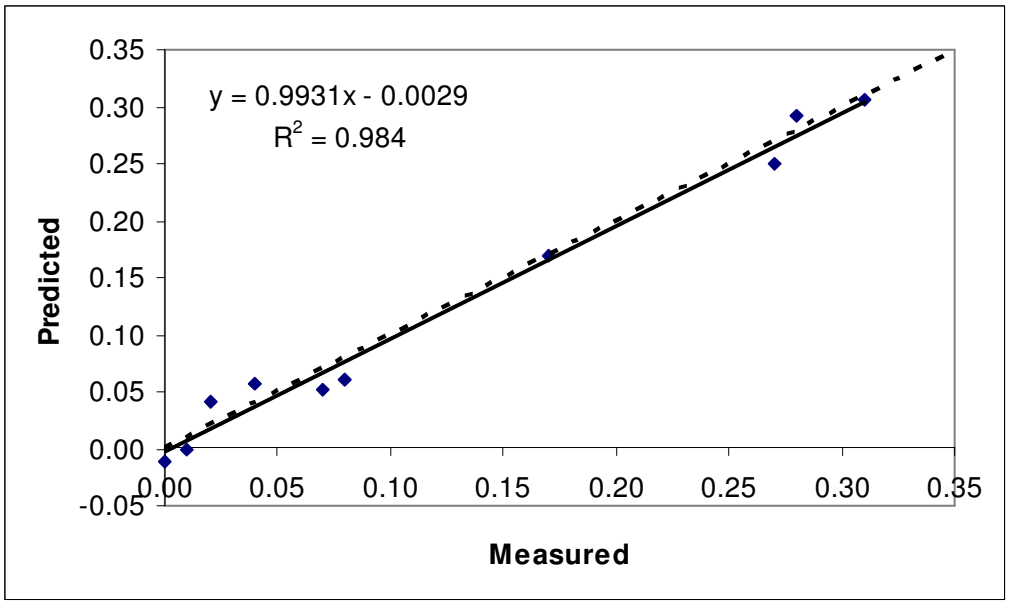

Fig. A19. Project 9-558-blend properties-
strain @ flow measured vs. predicted results

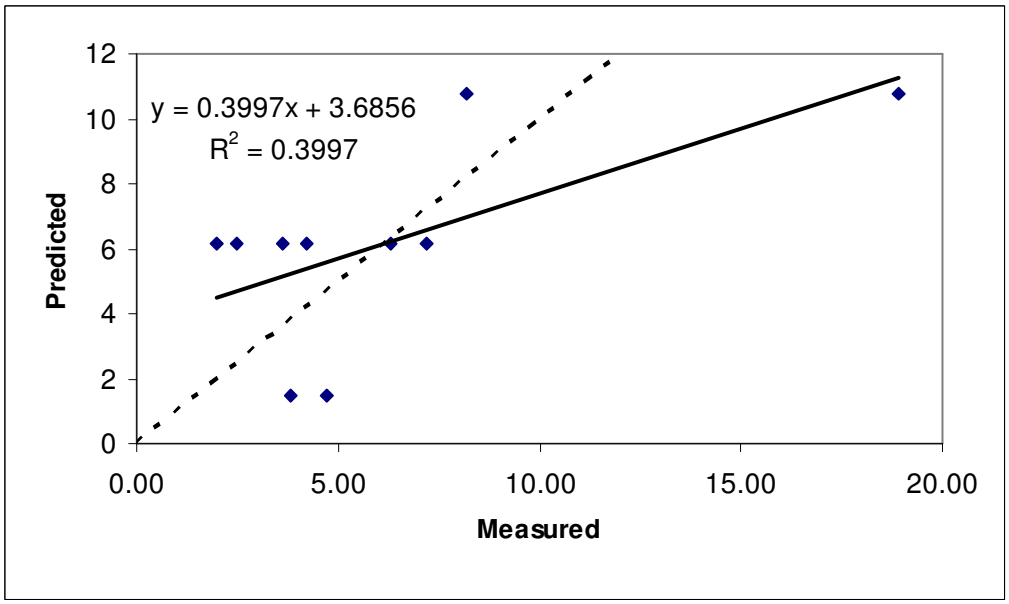

Fig. A20. Project 9-558-blend properties-
APA rut depth measured vs. predicted results

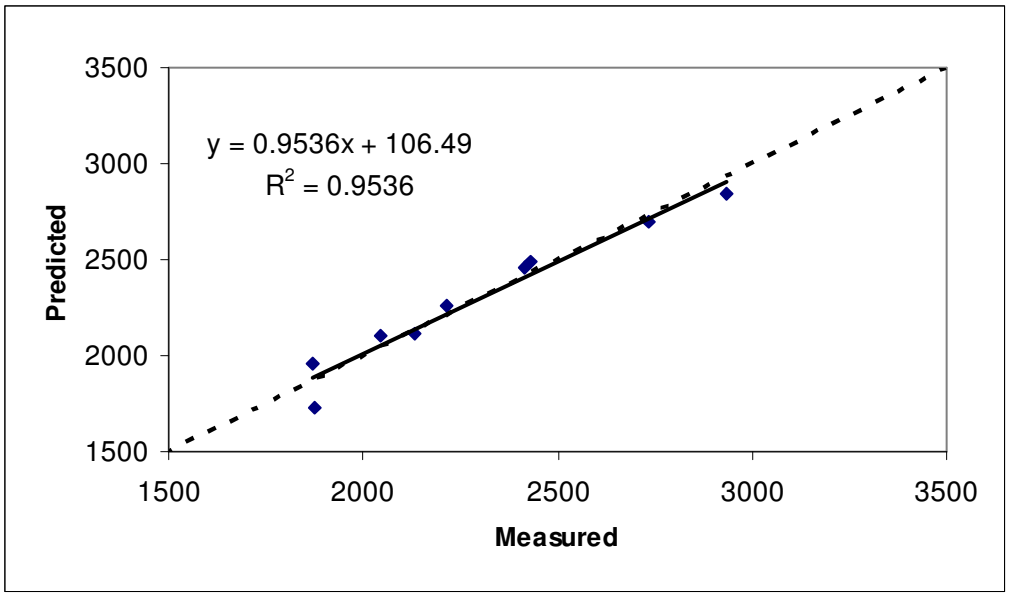

Fig. A21. Project 4203-average properties-
avg. E* at 5 Hz and 40°F measured vs. predicted results

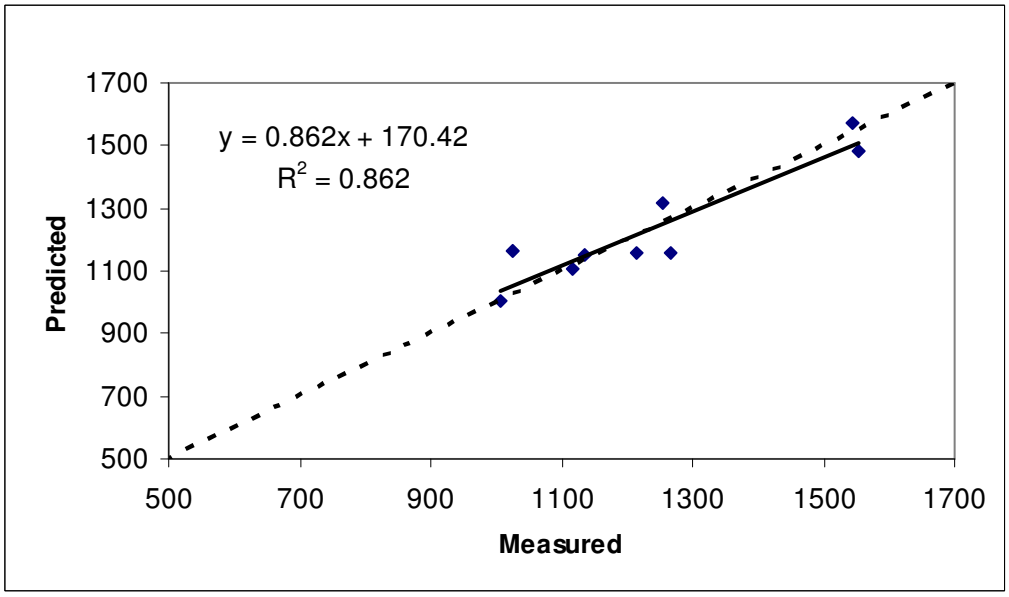

Fig. A22. Project 4203-average properties-
avg. E* at 5 Hz and 70°F measured vs. predicted results

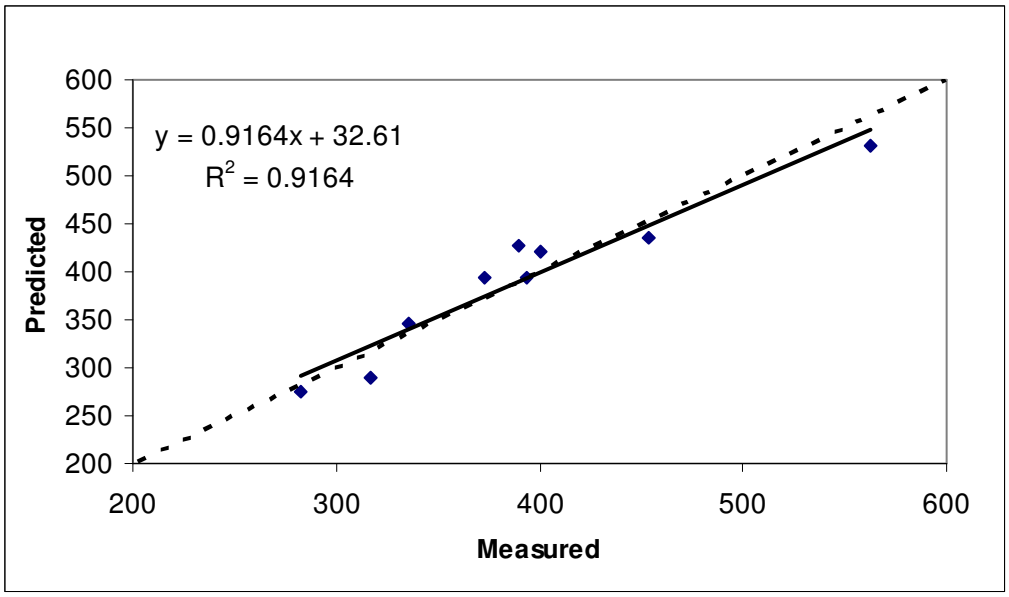

Fig. A23. Project 4203-average properties-
avg. E* at 5 Hz and 100°F measured vs. predicted results

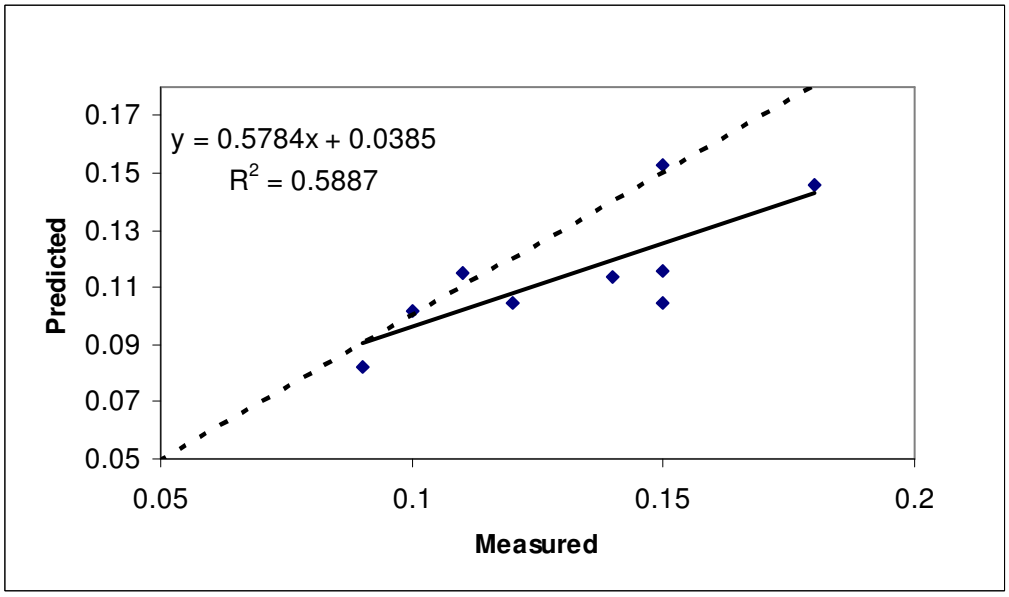

Fig. A24. Project 4203-average properties-
APA rut depth measured vs. predicted results

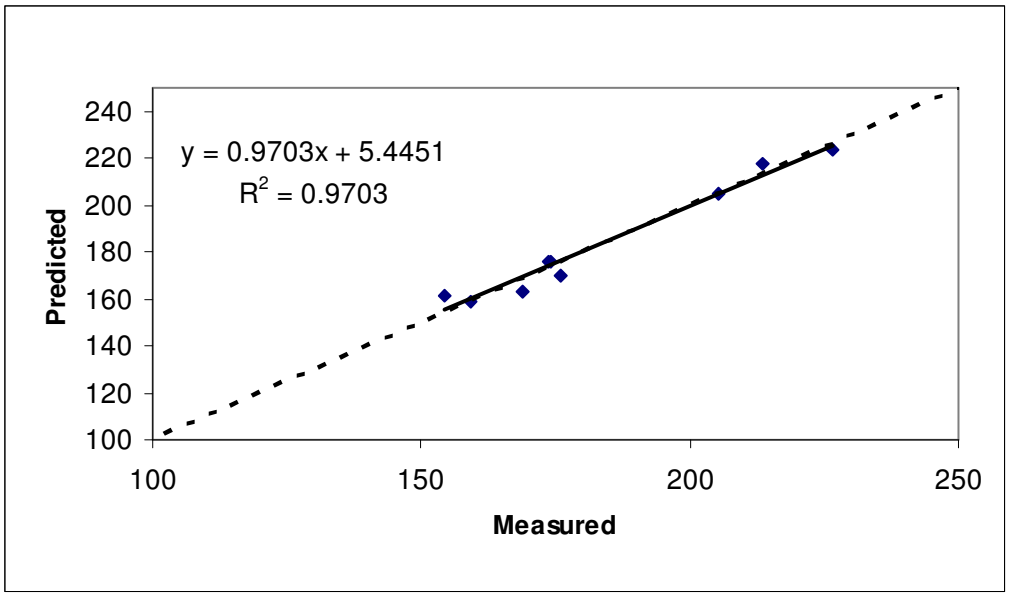

Fig. A25. Project 4203-average properties-
avg. IDT strength measured vs. predicted results

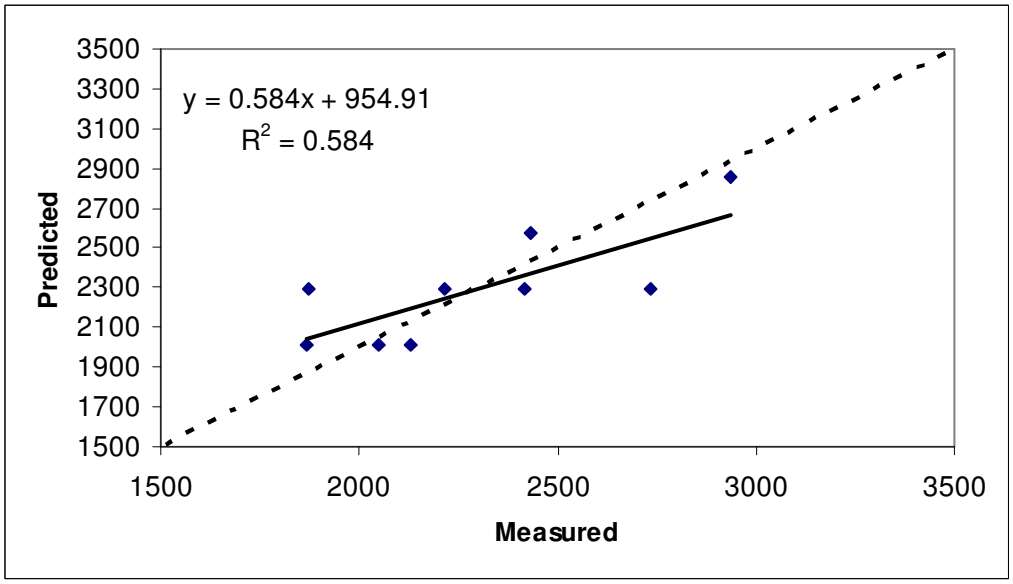

Fig. A26. Project 4203-blend properties-
avg. E* at 5 Hz and 40 ºF measured vs. predicted results

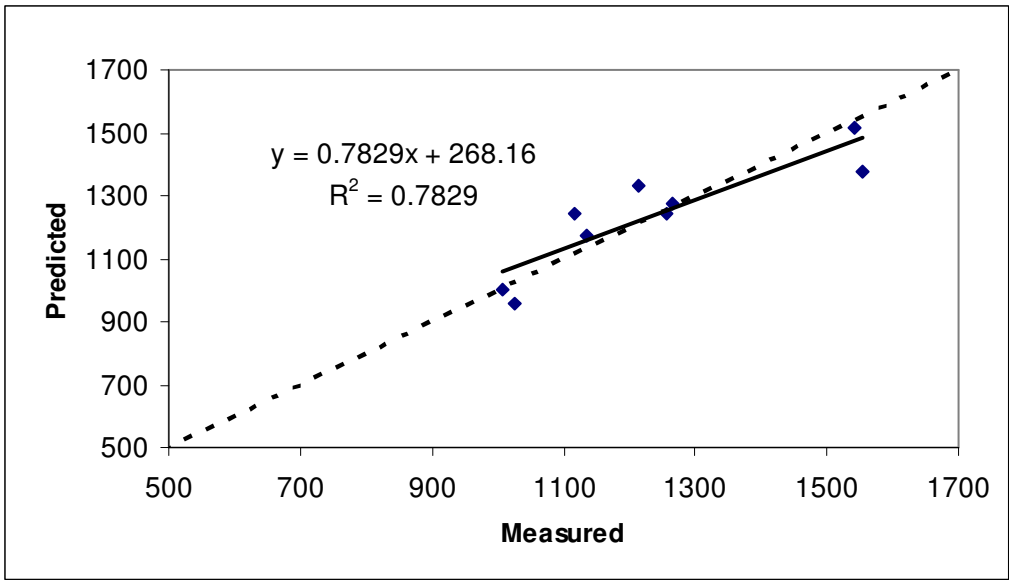

Fig. A27. Project 4203-blend properties-
avg. E* at 5 Hz and 70°F measured vs. predicted results

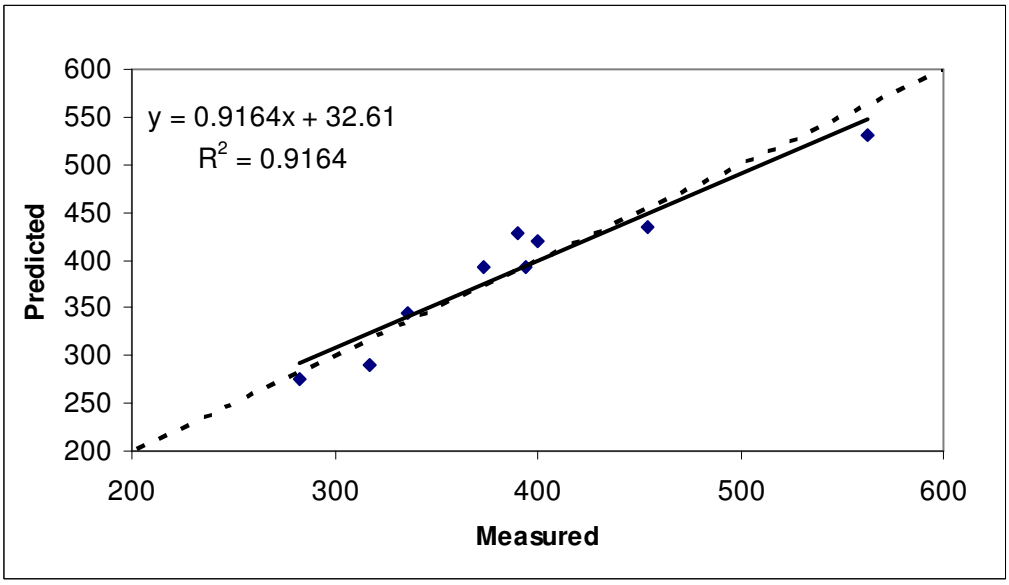

Fig. A28. Project 4203-blend properties-
avg. E* at 5 Hz and 100°F measured vs. predicted results

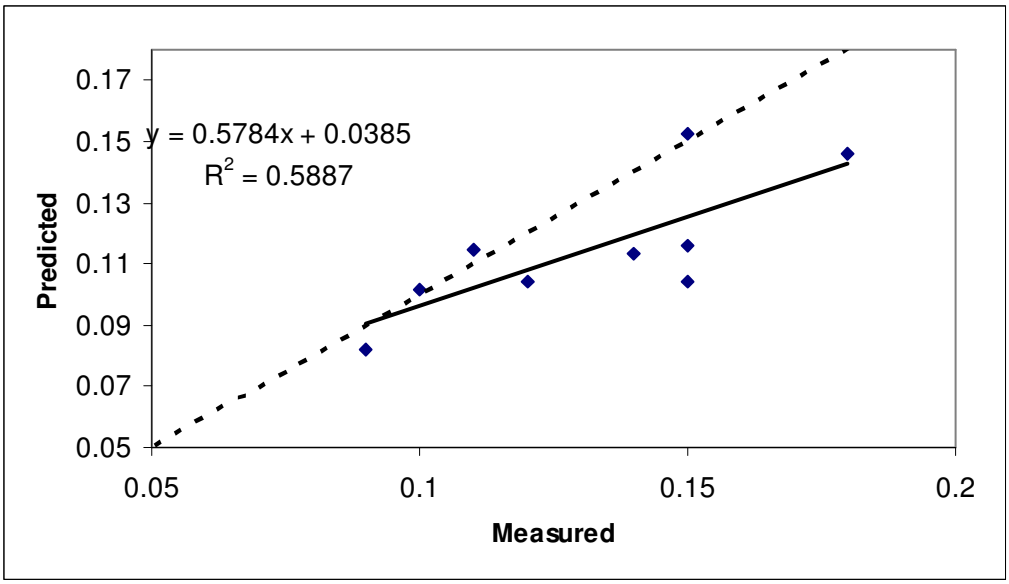

Fig. A29. Project 4203-blend properties-
APA rut depth measured vs. predicted results

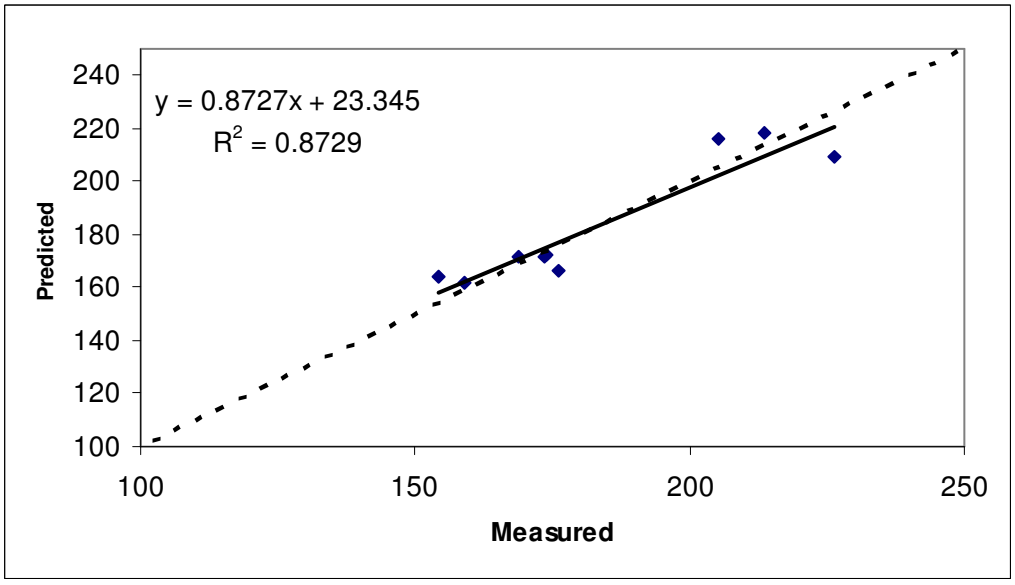

Fig. A30. Project 4203-blend properties-
avg. IDT strength measured vs. predicted results

VITA

Jeremy McGahan was born on February 18, 1981, in Ennis, Texas. He received his Bachelor of Science degree in civil engineering from Texas A&M University in December 2003, with specialization in structures. He then continued his education in January 2004, working on his Master of Science degree in civil engineering with specialization in materials. Jeremy worked as a research assistant at Texas Transportation Institute and as a teaching assistant for the Civil Engineering Department during his graduate studies. He graduated from Texas A&M University in December 2005 with a Master of Science degree in civil engineering.

Jeremy is currently residing at 717 Anthony Road, Ennis Texas, 75119. He can be contacted by email at jm_64@neo.tamu.edu. He can also be reached on his cell phone number at 979-739-2192.